

Reply to Anonymous Referee #1

We would like to thank you for the review and your constructive comments which help to improve the manuscript. We have revised the manuscript accordingly and our point-by-point responses (in blue) to the specific comments (in red) are given. The modification made in the manuscript is presented in green. This document also includes a marked-up version of manuscript.

Best Regards,
Soheila Jafariserajehlou

Comments to the Author:

1. Line 97: If you apply your algorithm to AATSR, clouds can change significantly in a period of 2 days quoted here as the return time.

- ✓ Author's response: We agree with the statements with respect to the changes of clouds in 2 days. In fact, these changes can help us to separate clouds (highly variable) from cloud-free surface (which could be considered as relatively stable in 2 days). We modified the text and explained more about the advantage of a shorter revisit time to our algorithm:
- ✓ Modifications: Line 104-108: In addition to multiple imagery over the Arctic, the shorter time interval between satellites over-passes over the same scene provides images with less variability in the observed cloud-free areas which the algorithm looks for. For the two SLSTR, the revisit time is 0.9 days at the equator (Coppo et al., 2010) and this time becomes even shorter at higher latitudes due to orbital convergence.

2. Line 162: What about continuity in the data record? There is a ~4 year gap between the failure of AATSR and the launch of SLSTR.

- ✓ Author's response: To fill this gap, we plan to apply the algorithm to the AVHRR measurements which have observations at the required wavelengths in ASCIA.
- ✓ Modifications: lines 180-183: However, there is a ~4 years gap between the failure of AATSR and the launch of SLSTR. To fill this gap, we will apply ASCIA also to the Advanced Very High Resolution Radiometer (AVHRR) sensor carried by National Oceanic and Atmospheric Administration (NOAA).

3. Line 250: The 11 micron BT although closest to surface temperature is not the 'real surface temperature' as it includes atmospheric effects. To give an example, LST or SST is never equal to BT in the 11 micron channel. If it were, we wouldn't need to retrieve surface temperature.

- ✓ Author's response: We agree. Actually, we meant the measured BT in the 11 micron channel is regarded to be in good agreement with the real surface temperature especially over snow and ice (Istomina et al., 2010; Musial et al., 2014). We corrected the sentence as below:

- ✓ Modifications: Line 271-274: This is estimated from observations at 11 μm where absorption by water vapor and other trace gases is small; most objects in regions outside of the tropics can be treated as blackbodies and the measured BT considered being in good agreement with real surface temperature (Istomina et al., 2010; Musial et al., 2014).

4. Line 312: Are you including all measurements within the block in the PCC calculation? This isn't clear in the text. If you are then your PCC is based on $\sim 25 \times 25$ pixels (x2 for two scenes?).

- ✓ Author's response: In this step we include all measurements (at 1.6 micron) within the block of 25×25 pixels in PCC calculation.
- ✓ Every PCC calculation is based on $\sim 25 \times 25$ pixels of two images. But the algorithm repeats PCC calculations between every two images unless all measurements in the time series are included. For one block of $\sim 25 \times 25$ pixels, PCC is calculated n times (n depends on the number of satellite overpass over the same scene). We explained this point at lines 330-332.

I would think in this scenario that most of the information is coming from the spatial variability rather than the temporal variability? If you are using a block average, this seems like too few observations to make a valid PCC calculation...

- ✓ In fact the information comes from spatial changes during the time. Therefore we believe both spatial and temporal variabilities contribute to this cloud detection algorithm. Since we do not have a single PCC to decide about one block of $\sim 25 \times 25$ pixels, instead we have PCC values over the time span. So we would say temporal variability and we would say it's not a block average.
- ✓ Modifications: Line 337-339: After computing the first binary cloud flag at block level using the last measurement and one previous image, ASCIA keeps the result in a memory and repeats the procedure with second previous data. This procedure is iterated until the last measurement of the data series is involved.

5. Line 335: New ice is also dark and I think you would find it hard to distinguish from open water. It would be good to mention this here too.

- ✓ Author's response: We appreciate this hint from the reviewer and added explanation about new ice to this part as below:
- ✓ Modifications: Line 361-362: Sea-ice is distinguished from water on the basis of its higher brightness; one scene might be white enough to be considered as ice. However, melting or broken ice as well as new ice would not be labeled as ice.

6. Making comparisons with SYNOP using a 45-minute time window for validation could be problematic? Clouds can move across a scene within minutes?

- ✓ In preparation of the article, we performed a comprehensive review of previous works to define the optimal maximum time difference. However, statements in literature strongly vary: 10 min (Werkmeister et al., 2015), 15 min (Musial et al., 2014), 1 h (Dybbroe et al., 2005) and 4 h (Meerkötter et al., 2004), obviously

all for different kinds of meteorological conditions. The investigation and results in the previous publications indicate that temporal difference in validation of satellite retrievals against SYNOP may vary based on meteorological conditions. Therefore we also tried to check meteorological conditions in our study.

- ✓ First, we checked to see which fraction of our results could be affected by longer temporal difference? We found that in 30% of our validation scenarios time difference exceeds half an hour. We tried to answer your question in these 30%. Do clouds change in the interval of 45 minutes? Or clouds could be almost stable due to the unique Arctic environment compared to lower latitudes? To answer this question we have performed two investigations:

1) We checked SYNOP data before and after validation time to see whether cloud changes could be observed during this time? Available to us were SYNOP data, i.e. cloud fraction every 3 hours over Svalbard and every 1 hour over Greenland. We found that only in 12% of our validation scenarios cloud fraction changed (± 1 or ± 2 oktas) within 2 hours (for Greenland) and – 6 hours (for Svalbard).

2) Another perspective on this topic is to ask how fast cloud can travel during our validation time window? We have checked the wind speed over Svalbard to answer the question. How strong the wind needs to be to move clouds out of or into in our validation area which is defined as a circle with the radius of 20 km around each SYNOP station? If we assume that the cloud is in the middle of this circle, we need at least a wind speed of 7.5 m/s to move clouds out of or into this circle in 45 minutes. Based on information from the Norwegian Meteorological Institute which provides an average of hourly wind speed, we see that the average wind speed over or close to the selected SYNOP stations at the closest stations during satellite overpass time is usually very low. For example below 3m/s and only in one scenario, it exceeds 7.5m/s slightly.

- ✓ Second, choosing a smaller temporal difference like for instance 0.5h would limit the number of observations and introduce a sampling error. For example, by filtering the validation dataset with respect to 0.5h temporal difference, 30% of the validation data will be lost. Therefore, to have a trade-off between good statistics/sampling and representativeness, we decided to keep the temporal interval of 45 minutes.
- ✓ However, temporal difference between satellite and SYNOP measurements is one of several sources of uncertainty (different viewing perspective, different spatial footprint etc.) which affect validation results. We have updated the text to address this comment and explain the uncertainty which originates from time difference.
- ✓ Modification: Line 465-477: To define the optimal maximum temporal difference between SYNOP and satellite data, other comparable validation activities used different temporal intervals like 10 min (Werkmeister et al., 2015), 15 min (Musial et al., 2014), 1 h (Dybbroe et al., 2005) and 4 h (Meerkötter et al., 2004). The investigation and results in the previous publications indicate that temporal difference in validation of satellite retrievals against SYNOP depend on meteorological conditions. Allowing only a

small temporal difference between measurement datasets (here: SYNOP and ASCIA) ensures an optimal temporal overall but can introduce a significant sampling error due to the small number of scenes for validation (Bojanowski et al., 2014). According to Bojanowski et al. (2014) a temporal difference of 90 min to compare with SYNOP measurements at temporal resolution of 3 h minimizes the sampling error (Bojanowski et al., 2014). However, potential longer temporal difference will introduce an error which should be considered along other sources of uncertainty (different viewing perspective, different spatial footprint and etc.). In this study, the maximum allowed temporal difference between the ASCIA retrievals and SYNOP measurements is less than ± 20 minutes in most cases and generally does not exceed ± 45 minutes.

- ✓ Line 558: Bojanowski, J., Stöckli, R., Tetzlaff, A., and Kunz, H.: The Impact of Time Difference between Satellite Overpass and Ground Observation on Cloud Cover Performance Statistics, *Remote Sensing*, 6, 12 866–12 884, <https://doi.org/10.3390/rs61212866>, 2014.
- ✓ Line 575: Dybbroe, A., Karlsson, K.-G., Thoss, A., NWCSAF AVHRR cloud detection and analysis using dynamic thresholds and radiative transfer modeling. Part II: Tuning and validation. *J. Appl. Meteorol.*, 44, 55–71, 2005.
- ✓ Line 640: Meerkötter, R., König, C., Bissolli, P., Gesell, G., Mannstein, H., A 14-year European cloud climatology from NOAA/AVHRR data in comparison to surface observations. *Geophys. Res. Lett.*, 31, doi:10.1029/2004GL020098, 2004.

7. *Please check the use of English throughout. The manuscript is readable but often the sentence structure isn't quite right and this makes it more difficult to understand. To give an example (line 222): o Manuscript: 'One major contributors of error in aerosol retrieval is misclassifying heavy aerosol loads with clouds.' o Correct English: 'One of the major contributors to error in aerosol retrievals is misclassification of heavy aerosol loads as cloud.'

- ✓ Author's response: Done.
- ✓ Modifications: Line 244-245: One of the major contributors to error in aerosol retrievals is misclassification of heavy aerosol loads as cloud.
- ✓ We also check the whole manuscript.

8. The structure of the text within the various sections of the manuscript could be improved/tightened up in places, particularly in the introduction.

- ✓ Done.

9. Figures 1-2, 5-13: It would be good to enlarge all of these figures so that they are more readable and cloud/surface features can be identified.

- ✓ Done; all figures are enlarged.

10. Figures 1-2, 5-13: It is far more intuitive for the reader if cloud is white and clear-sky is black. Colours should also match between algorithms. For example in one plot you have black=cloud, white=clear, and in another white=snow. This can become quite confusing for the reader to interpret.

- ✓ Done. Thanks for pointing out this issue. The figures (5-13) have been updated and they are more intuitive for the reader now. But in figures 1-2, we used different color schemes to highlight different features such as temperature (not only cloud information) observed at various wavelengths.

11. Table 4: The use of the terms ‘correct’ and ‘incorrect’ here assumes that there is no uncertainty in the SYNOP data. Is this really true? How are the oktas determined from this data? Does it involve human input? Is misclassification possible? I would be inclined to use the terms ‘agreement’ and ‘disagreement’ with the caveat that SYNOP isn’t perfect made within the text.

- ✓ Done. We agree. The use of “correct” term is not suitable, as you mentioned, the measurements involve human input. Actually, we explained this uncertainty involved in these observations at lines 196-198. We changed the word correct and incorrect to agreement and disagreement.
- ✓ Modifications: line 714.

Cloud data	Criteria	
	within ± 2 oktas	within ± 1 okta
ASCIA vs. SYNOP	96 % agreement 4 % disagreement	83 % agreement 17 % disagreement
ESA vs. SYNOP	68 % agreement 32 % disagreement	50 % agreement 50 % disagreement

12. Figures with RGB: Are these actual RGB’s or false colour images? This should be made clear and the channels used described in the figure captions.

- ✓ They are false colour images. We used 0.67, 0.87 and 0.55 μm channels. We added this information to figure captions.

13. Figure 16: Light blue error bars are difficult to see. Could you change the colour?

- ✓ Done.

14. There is some existing literature about cloud detection and surface classification over Polar Regions from within the SST CCI project: o Bulgin, C. E., Eastwood, S., Embury, O., Merchant, C. J. and Donlon, C. (2015) Sea surface temperature climate change initiative: alternative image classification algorithms for sea-ice affected oceans. Remote Sensing of Environment, 162. pp. 396-407. ISSN 0034-4257 doi: <https://doi.org/10.1016/j.rse.2013.11.022> How does your algorithm compare to a Bayesian approach? This paper also shows the limitations of the SADIST mask that you mention in your paper.

- ✓ We read the above mentioned paper from Bulgin et al. (2015). The work aims to discriminating clear-sky ice-free ocean. Though these two algorithms (Bulgin et al. (2015) and this work) are different methods, there are some similarities in the general ideas of both algorithms. For example, we used similar

wavelengths (3.7, 1.6, 0.6 μm). Based on our investigation, the combination of the selected bands can improve the accuracy of snow/ice, cloud and ocean discrimination; similar conclusion can be found in Bulgin et al. (2015). The benefits can be increased when spectral and textural modification using the texture derived from 1.6 μm is employed. Additionally we also concluded that using temperature information alone, could lead to significant misclassification over Polar Regions as Bulgin et al. (2015) indicated.

- ✓ Both algorithms have their advantages and disadvantages. The advantageous of Bulgin et al. (2015) is that the algorithm has been optimized of the algorithm for night/twilight time. The advantageous of our algorithm is: it can be used over land covered by snow/ice along Open Ocean.
- ✓ We added the mentioned paper to our references as below:
- ✓ Modification: line 67-69: SADIST is known to misclassify ice, cloud and open ocean in Polar Regions. Bulgin et al. (2015) developed a Bayesian approach in ESA's Climate Change Initiative (CCI) project to overcome this limitation (Hollmann et al., 2013).
- ✓ Line 561-563: Bulgin, C. E., Eastwood, S., Embury, O., Merchant, C. J. and Donlon, C., Sea surface temperature climate change initiative: alternative image classification algorithms for sea-ice affected oceans. Remote Sensing of Environment, 162, pp. 396-407, 2015.
- ✓ Line 593-595: Hollmann, R.; Merchant, C.J.; Saunders, R.; Downy, C.; Buchwitz, M.; Cazenave, A.; Chuvieco, E.; Defourny, P.; de Leeuw, G.; Forsberg, R.; et al. The ESA climate change initiative Satellite Data Records for Essential Climate Variables. Bull. Am. Meteorol. Soc., 94, 1541–1552, 2013.

15. Have you given any consideration to classification at nighttime? I realise that in the context of aerosol retrievals this isn't relevant, but it is for other applications so would be good to include a sentence on this.

- ✓ We did not consider cloud identification at night time yet. As you already mentioned the aim of this work was masking clouds for aerosol retrieval. However, we may have such improvements in the next version of this algorithm. We modified the text as below:
- ✓ Modifications: Line 537-539: The objective of this study was to assess and validate the current version of ASCIA for daytime observations. For night time application, an adaption of ASCIA is planned to identify clouds during night.

Technical comments:

1. Line 32: Comma after 'though' doesn't make sense.

- ✓ Done.
- ✓ Modifications: Line 33: Though the attribution of the origins this phenomenon is ...

2. Line 36: Comma after 'since' doesn't make sense. Please check throughout, as there are not many instances in English where it is appropriate to use a comma after the first word in a sentence, except with 'however' on occasion.

- ✓ Done.

- ✓ Modifications: Line 37: Since all developed cloud detection methods encounter many obstacles originating from the unique atmosphere and surface conditions in the Arctic (Curry et al., 1996).

3. Line 39: Snow/ice are also cold – this is the limiting factor in the thermal infrared.

- ✓ Done.
- ✓ Modifications: Line 40-42: For example, snow/ice are also like clouds cold, the lack of strong thermal contrast is a limitation in the retrieval of clouds in the thermal infrared (Rossow and Garder 1993; Curry et al., 1996).

4. Line 47: ‘as’ thin cloud?

- ✓ Done.
- ✓ Modifications: Line 49: To avoid the uncertainty included in AOT products due to significant misclassification of heavy aerosol load as thin cloud...

5. Line 151/152: The revisit times stated here are not consistent with those given in the introduction (0.9 days).

- ✓ Done.
- ✓ Modifications: Line 166-167: This yields global revisit times of 1.9 days at the equator with two satellites and 0.9 day with one satellite.

6. Line 277: Only in Polar Regions – deserts for example can be bright. Sunlint over water is also bright.

- ✓ Done.
- ✓ Modifications: Line 299: This is because land scenes in Polar region are dark in comparison to cloud and snow.

7. Line 650: Should be ‘lower’.

- ✓ Done.
- ✓ Modifications: Line 722: (lower panels)

Reply to Anonymous Referee #2

We would like to thank you for the review and your constructive comments which help to improve the manuscript. We have revised the manuscript accordingly and our point-by-point responses (in blue) to the specific comments (in red) are given. The modification made in the manuscript is presented in green. This document also includes a marked-up version of manuscript.

Best Regards,
Soheila Jafariserajehlou

Comments to the Author:

Reviewer #2: Please check you English. The content of the paper really suffer from lack of structure, wrong grammar and misplaced commas. Also, you should not use an article before ASCIA, except when it is used as adjective. Example: “ASCIA retrieves clouds over Artic” or “The ASCIA retrieval over Artic”. This is true for all acronyms and abbreviations (e.g. SLSTR). Since (which certainly does not require a comma) introduces a subordinate sentence, which cannot be separated from the main clause by a full stop.

- ✓ We have corrected all these points throughout the manuscript.

Reviewer #2: It is not clear to me whether or not your algorithm is applicable during winter. At line 357 you write that your targeted seasons are spring, summer and autumn and then you choose March, May and July. This is already confusing by itself. Later, at line 362 you write that ASCIA is not optimized for winter time. Could you please clarify this?

- ✓ We are sorry for this inaccurate statement. The algorithm is not optimized for night time retrievals (the information from the visible channels may not be valid during night) and we do not attempt to apply it during polar night. In fact, we only had access to 3 months (March, May and July) of SYNOP data which we used for validation. We understood the confusion arising from this statement and it would be better not to mention seasons here. We modified the text as below:
- ✓ Modification: Line 388- 395: Three months of data from March, May, and July have been acquired over Greenland and Svalbard to assess the performance of ASCIA in a wide range of solar zenith angles (60°- 85°), surface and atmospheric conditions observed at high latitudes. In order to take various surface types in the Arctic into account, we selected case studies including, highly variable topography and fairly homogeneous snow cover, coast lines, land and ocean along snow and ice covered surface. The designed criteria for ASCIA are optimized for various regions over the Arctic observed under different solar illumination conditions. Polar night and transition seasons at low light conditions are excluded from our retrievals.

Reviewer #2: Fig. 5 The left panel over Greenland shows 2 rectangles in left part of the image. Could you please discuss where they arise from? Your algorithm shows promising results, but it is always worthwhile to discuss its limitations.

✓ We see these rectangles on the middle and right panels over Greenland:

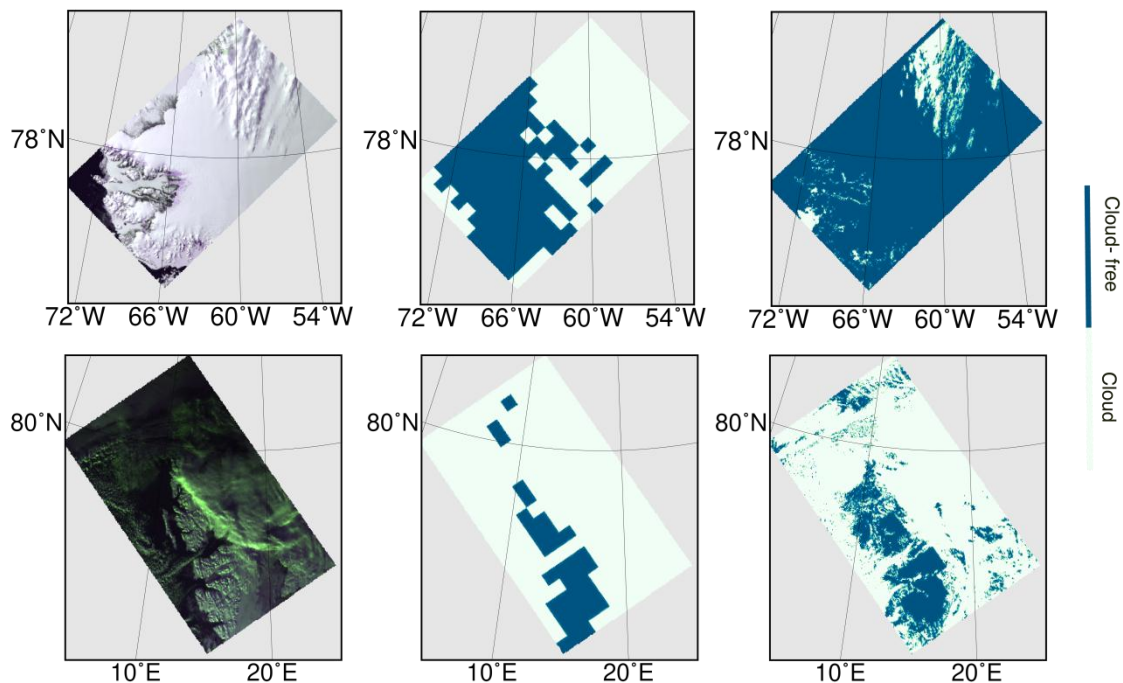
Middle panel: In the middle panel, these 2 rectangles are indicators of the blocks with low Pearson Correlation Coefficient (PCC smaller than 0.4). As we can see from the corresponding RGB image, the locations of these two rectangles are over/near open water. We already discussed this shortcoming of the PCC analysis at lines 322-325 (in the original version of this manuscript): “Small PCC values may be caused by rapid surface change, high aerosol load or lack of recognizable spatial pattern, which is often the case over homogeneous snow covered surface”. Therefore the lack of geo-physical patterns and structure could be a potential reason in this case. We also mentioned at lines 318-319 in the original version of manuscript “The combination of these two constraints is necessary because neither PCC analysis nor the reflectance part of $3.7 \mu\text{m}$ is adequate on its own for accurate cloud detection”.

Right panel: However, using the reflectance of $3.7 \mu\text{m}$ compensates the limitation of the PCC criterion as we explained at line 393-396. As we can see in the final results of this image (in Fig. 12 in the results section) these two rectangles over open water disappeared. Therefore the right panel in Fig. 5 (in original version of the manuscript) should not have these rectangles as well.

We thank the referee for this information. We realized that we have used erroneously an outdated version of this picture (which was not created using the right running version of the algorithm).

We have updated the right panel in Fig. 5 (with an improved color scheme (comment from the reviewer #1)). Please see below.

✓ Modification: Line 721 Fig. 5.



Reviewer #2: L398 You say the computing time is higher. How higher? Please give an estimate.

- ✓ The run-time of one scene is 30 minutes on a state-of-the-art computer system.

Reviewer #2: L428 I agree with the other reviewer, 45 minute time difference seem to me quite large for validation purposes. Maybe you should introduce a filtering?

- ✓ In preparation of the article, we performed a comprehensive review of previous works to define the optimal maximum time difference. However, statements in literature strongly vary: 10 min (Werkmeister et al., 2015), 15 min (Musial et al., 2014), 1 h (Dybbroe et al., 2005) and 4 h (Meerkötter et al., 2004), obviously all for different kinds of meteorological conditions. The investigation and results in the previous publications indicate that temporal difference in validation of satellite retrievals against SYNOP may vary based on meteorological conditions. Therefore we also tried to check meteorological conditions in our study.
- ✓ First, we checked to see which fraction of our results could be affected by longer temporal difference? We found that in 30% of our validation scenarios time difference exceeds half an hour. We tried to answer your question in these 30%. Do clouds change in the interval of 45 minutes? Or clouds could be almost stable due to the unique Arctic environment compared to lower latitudes? To answer this question we have performed 2 investigations:
 - 1) We checked SYNOP data before and after validation time to see whether cloud changes could be observed during this time? Available to us were SYNOP data, i.e. cloud fraction every 3 hours over Svalbard and every 1 hour over Greenland. We found that only in 12% of our validation scenarios cloud fraction changed (± 1 or ± 2 oktas) within 2 hours (for Greenland) and – 6 hours (for Svalbard).
 - 2) Another perspective on this topic is to ask how fast cloud can travel during our validation time window? We have checked the wind speed over Svalbard to answer the question. How strong the wind needs to be to move clouds out of or into in our validation area which is defined as a circle with the radius of 20 km around each SYNOP station? If we assume that the cloud is in the middle of this circle, we need at least a wind speed of 7.5 m/s to move clouds out of or into this circle in 45 minutes. Based on information from the Norwegian Meteorological Institute which provides an average of hourly wind speed, we see that the average wind speed over or close to the selected SYNOP stations at the closest stations during satellite overpass time is usually very low. For example below 3m/s and only in one scenario, it exceeds 7.5m/s slightly.
- ✓ Second, choosing a smaller temporal difference like for instance 0.5h would limit the number of observations and introduce a sampling error. For example, by filtering the validation dataset with respect to 0.5h temporal difference, 30% of the validation data will be lost. Therefore, to have a trade-off between good statistics/sampling and representativeness, we decided to keep the temporal interval of 45 minutes.
- ✓ However, temporal difference between satellite and SYNOP measurements is one of several sources of uncertainty (different viewing perspective, different spatial footprint etc.) which affect validation results.

We have updated the text to address this comment and explain the uncertainty which originates from time difference.

- ✓ Modification: Line 465-477: To define the optimal maximum temporal difference between SYNOP and satellite data, other comparable validation activities used different temporal intervals like 10 min (Werkmeister et al., 2015), 15 min (Musial et al., 2014), 1 h (Dybbroe et al., 2005) and 4 h (Meerkötter et al., 2004). The investigation and results in the previous publications indicate that temporal difference in validation of satellite retrievals against SYNOP depend on meteorological conditions. Allowing only a small temporal difference between measurement datasets (here: SYNOP and ASCIA) ensures an optimal temporal overall but can introduce a significant sampling error due to the small number of scenes for validation (Bojanowski et al., 2014). According to Bojanowski et al. (2014) a temporal difference of 90 min to compare with SYNOP measurements at temporal resolution of 3 h minimizes the sampling error (Bojanowski et al., 2014). However, potential longer temporal difference will introduce an error which should be considered along other sources of uncertainty (different viewing perspective, different spatial footprint and etc.). In this study, the maximum allowed temporal difference between the ASCIA retrievals and SYNOP measurements is less than ± 20 minutes in most cases and generally does not exceed ± 45 minutes.
- ✓ Line 558: Bojanowski, J., Stöckli, R., Tetzlaff, A., and Kunz, H.: The Impact of Time Difference between Satellite Overpass and Ground Observation on Cloud Cover Performance Statistics, Remote Sensing, 6, 12 866–12 884, <https://doi.org/10.3390/rs61212866>, 2014.
- ✓ Line 575: Dybbroe, A., Karlsson, K.-G., Thoss, A., NWCSAF AVHRR cloud detection and analysis using dynamic thresholds and radiative transfer modeling. Part II: Tuning and validation. J. Appl. Meteorol., 44, 55–71, 2005.
- ✓ Line 640: Meerkötter, R., König, C., Bissolli, P., Gesell, G., Mannstein, H., A 14-year European cloud climatology from NOAA/AVHRR data in comparison to surface observations. Geophys. Res. Lett., 31, doi:10.1029/2004GL020098, 2004.

Reviewer #2: Sections Results and Validation could be compressed in one section, as even when presenting the results you do some qualitative validation against other cloud products.

- ✓ Done.

Reviewer #2: L454 Could you please show part of the evaluation against AERONET? AS the latter is a well-known reference for every reader, the validation against it deserves more than 2 lines of text. Also, which version are you using? And why L1.5 instead of L2.0?

- ✓ We agree and modified the text as below. Unfortunately it was not possible to perform further statistical analysis (like we did for SYNOP) in validation against AERONET because the comparison is pixel-based and does not include a circular area around the station where we could estimate cloud fraction.
The reason for selecting level 1.5 instead of level 2.0 is that, level 1.5 data are cloud screened but level 2.0 data are quality assured. This means if we use level 1.5 data and check whether we have aerosol

measurements or not (having aerosol measurements means cloud-free condition) we could have information of cloudiness. But, in level 2.0 data, missing aerosol data could also be due to low quality of measurements.

- ✓ Modification: Line: 504-508: We also validated ASCIA cloud identification results with AERONET level 1.5 measurements, which are cloud screened. The procedure for this validation takes place in 2 steps: (1) covering AERONET observed AOT to a cloud flag (AOT is provided in AERONET only in cloud-free conditions); (2) Validation of ASCIA with AERONET cloud flag. In 86.1 % of 36 studied scenes over Svalbard, both ASCIA and AERONET confirm the presence of clouds.
- ✓ Reviewer #2: Technical comments L151 The SLSTR revisit time is 1.9 day at the equator with one satellite and 0.9 day with two satellites, not single/dual view.
- ✓ Done.
- ✓ Modification: lines 166-167: This yields global revisit times of 1.9 days at the equator with two satellites and 0.9 day with one satellite.

Reviewer #2: Table 3. The title of the second column should be something like “Test”

- ✓ Done.
- ✓ Modification: line 712.

Surface Type	Test	Description
Water	$R_{0.87} < 11\% \ \& \ NDSI \geq 0.4$	MODIS snow and ice mapping ATBD
Sea-ice	$R_{0.87} > 11\% \ \& \ NDSI \geq 0.4$	(Hall et al., 2001)
Land	$R_{3.7} > 0.04 \ \& \ R_{0.66} < 0.2 \ \ NDSI < 0.4$	Allen et al., 1999
Snow	$R_{3.7} \leq 0.04$	Allen et al., 1999

Reviewer #2: Figures 1-2, fig. from 5 to 13 and fig. 16 should indeed be larger.

- ✓ Done.

Reviewer #2: L339-347 please simplify these lines. Throughout your manuscript sentences are often too long, but here they really affect the readability. Simplify the lines here and maybe add more information on the caption of the figures (for example the exact coordinates of the corners)

- ✓ Done.
- ✓ Modification: line 365-370: A representative example of the block level (25×25 km²) and scene level (1×1 km²) results of ASCIA applied to AATSR observations is shown in Fig. 5. This example was selected to show the performance of ASCIA in presence of different surface conditions: 1) one scene is over a combination of fairly homogenous snow cover, land, ocean, sea-ice and cloud scene at north-west of

Greenland taken on the 18 May 2008; 2) another example is over a surface with highly variable topography over Svalbard with relatively higher solar zenith angle ($>80^\circ$) on the 1 March 2008.

- ✓ Line 707-711: Figure 5. Examples of the results of ASCIA on AATSR observations on the scenes over Greenland (upper panels) between (75°N, 48°W), (75°N, 75°W), (81°N, 48°W), (81°N, 75°W), taken on the 18 May 2008 and Svalbard (lower panels) within (75°N, 4°E), (75°N, 32°E), (81°N, 4°E), (81°N, 32°E) (lower panels), on the 1 March 2008, Left panels: RGB images, middle panels: Cloud detection at block level (25×25 km²), right panels: cloud detection at scene level.

Reviewer #2: L16 reflection at 3.7 um

- ✓ Done.
- ✓ Modification: line 16: Subsequently, the reflection at 3.7 μ m is used for accurate cloud identification at...

Reviewer #2: L18 e.g. e.g.

- ✓ Done.
- ✓ Modification: line 17: The ASCIA data product has been validated by comparison with independent observations e.g. surface synoptic observations (SYNOP)

Reviewer #2: L32 Though the attribution of the origins of this phenomenon

- ✓ Done.
- ✓ Modification: line 33: Though the attribution of the origins of this phenomenon is controversially discussed.

Reviewer #2: L76 the aim is

- ✓ Done.
- ✓ Modification: line 82: ... where the aim is to simultaneously retrieve aerosol and surface properties.

Reviewer #2: L104 it is also planned to apply it to the observations acquired by SLSTR

- ✓ Done.
- ✓ Modification: line 115-116: It is also planned to apply it to the observations acquired by SLSTR onboard Sentinel-3A and Sentinel-3B launched in 2016 and 2018 respectively which provide continuity of AATSR observations.

Reviewer #2: L123 In the upper right

- ✓ Done.
- ✓ Modification: line 137: For example, in the upper right panel...

Reviewer #2: L131 Each scene is

- ✓ Done.
- ✓ Modification: line 145: Each scene is imaged twice.

Reviewer #2: L142 These algorithms are typically not optimized

- ✓ Done. We deleted this line.

Reviewer #2: L168 For example, they are almost absent in the central parts

- ✓ Done.
- ✓ Modification: line 188-189: For example, there is almost no observation in the central parts of the Arctic Circle as is shown in Fig. 3.
- ✓ Reviewer #2: L187 AERONET is . . .
- ✓ Done.
- ✓ Modification: line 208: AERONET is a network of approximately 700 ground-based sun photometers established by National Aeronautics and Space Administration (NASA) and PHOTométrie pour le Traitement Opérationnel de Normalisation Satellitaire (PHOTONS).

Reviewer #2: L206 Then the PCC can be written as

- ✓ Done.
- ✓ Modification: line 226-228: To describe the computational procedure developed, we assume x , y to be two random variables, then the PCC can be written as a function of the covariance...
- ✓ Reviewer #2: L207 function of the covariance
- ✓ Done.
- ✓ Modification: line 228: ... then the PCC can be written as a function of the covariance...
- ✓ Reviewer #2: L241 no new line
- ✓ Modification: line 264.
- ✓ Done.

Reviewer #2: L254 Here you should compact everything in one sentence

- ✓ Done.
- ✓ Modification: line 278-281: where $R_{3.7}$ is the reflectance i.e. the ratio of scattered radiance to incident solar radiance; L measured radiance at $3.7 \mu\text{m}$, $B_{3.7}(T_{11})$ the Planck function radiance (the contribution from thermal emission at $3.7 \mu\text{m}$) T_{11} measurements at $11 \mu\text{m}$; $F_{3.7,0}$ the solar constant at $3.7 \mu\text{m}$ and μ_0 the cosine of solar zenith angle.

Reviewer #2: L285 AATSR provides

- ✓ Done.
- ✓ Modification: line 309: AATSR provides more data over higher latitudes, ...

Reviewer #2: L310 found that a PCC of 06

- ✓ Done.
- ✓ Modification: line 334-336: ...we defined a lower threshold for PCC of 0.4 over the Arctic region and found that a PCC of 0.6 is appropriate for middle latitudes based on a number of statistical analyses.

Reviewer #2: L319 ASCIA starts looking for remaining small cloud scenes within a block, i.e. scenes . . . (R3.7 > 0.04)

- ✓ Done.
- ✓ Modification: line 346: ASCIA starts looking for remaining small cloud scenes within a block, i.e. scenes with $R_{3,7}$...

Reviewer #2: L333 it is important to note that one scene, . . .

- ✓ Done. We changed this sentence.
- ✓ Modification: line 359: Although characterized as land, a scene may include soil, different types of vegetation cover or even melting snow.

Reviewer #2: L334 The latter mix with soil and becomes

- ✓ Done.
- ✓ Modification line 360: The latter mix with soil and becomes dark enough to be filtered out from the snow class. Sea-ice is distinguished from water on the basis of its greater brightness...

Reviewer #2: L339 a representative example

- ✓ Done.
- ✓ Modification: line 365: A representative example of the block level ($25 \times 25 \text{ km}^2$) and scene level ($1 \times 1 \text{ km}^2$) results of ASCIA...

Reviewer #2: L373 cloud free scene which ISTO failed to detect but are correctly labeled by ASCIA.

- ✓ Done.
- ✓ Modification: line 406: The reddish scenes show cloud free cases, which ISTO fails to detect, but are correctly labeled by ASCIA as cloud free.

Reviewer #2: L393 Both the ESA and ISTO

- ✓ Done.
- ✓ Modification line 426: Both the ESA and ISTO cloud products showed good results for this case with the exception of thin cloud scenes which are falsely labeled as clear snow by ISTO.

Reviewer #2: L447 would be expected from SYNOP

- ✓ Done.
- ✓ Modification: line 497: As discussed earlier an error of ± 1 to ± 2 okta would be expected as the accepted accuracy range from SYNOP cloud cover values due to man-made nature of its observation and viewing conditions.

A cloud identification algorithm over the Arctic for use with AATSR/SLSTR measurements

Soheila Jafariserajehlou¹, Linlu Mei¹, Marco Vountas¹, Vladimir Rozanov¹, John P. Burrows¹, Rainer Hollmann²

¹Institute of Environmental Physics, University of Bremen, Otto-Hahn-Allee 1, Bremen, 28359, Germany

²DWD – Deutscher Wetterdienst, Frankfurter Straße 135, 63067 Offenbach, Germany

Correspondence to: Soheila Jafariserajehlou (jafari@iup.physik.uni-bremen.de)

Abstract. The accurate identification of the presence of cloud in the ground scenes observed by remote sensing satellites is an end in itself. ~~The~~ lack of knowledge of cloud at high latitudes increases the error and uncertainty in the evaluation and assessment of the changing impact of aerosol and cloud in a warming climate. A prerequisite for the accurate retrieval of Aerosol Optical Thickness, AOT, is the knowledge of the presence of cloud in a ground scene.

In this study observations of the upwelling radiance in the visible (VIS), near infrared (NIR), shortwave infrared (SWIR), and the thermal infrared (TIR), coupled with solar extraterrestrial irradiance are used to determine the reflectance. We have developed a new cloud identification algorithm for application to the reflectance observations of Advanced Along-Track Scanning Radiometer (AATSR) on European Space Agency (ESA)-Envisat and Sea and Land Surface Temperature Radiometer (SLSTR) onboard the ESA Copernicus Sentinel-3A and -3B. The resultant AATSR/SLSTR Cloud Identification Algorithm (ASCIA) ~~developed~~ addresses the requirements for the study AOT at high latitudes and utilizes time-series measurements. It is assumed that cloud free surfaces have unchanged or little changed patterns for a given sampling period, whereas cloudy or partly cloudy scenes show much higher variability in space and time. In this method, the Pearson Correlation Coefficient (PCC) parameter is used to measure the ‘stability’ of the atmosphere-surface system observed by satellites. The cloud free surface is classified by analyzing the PCC values at the block scale $25 \times 25 \text{ km}^2$. Subsequently, the reflection ~~at~~ $3.7 \mu\text{m}$ is used for accurate cloud identification at ~~the~~ scene level: ~~having areas of~~ -either $1 \times 1 \text{ km}^2$ or $0.5 \times 0.5 \text{ km}^2$. The ASCIA data product has been validated by comparison with independent observations e.g. ~~s~~Surface synoptic observations (SYNOP), ~~the data from~~ AEROSOL ROBOTIC NETWORK (AERONET) and the following satellite-products ~~from~~ i) ~~The~~ ESA standard cloud product from AATSR L2 nadir cloud flag; ii) ~~The product from a one~~-method based on clear-snow spectral shape developed at IUP Bremen (Istomina et al., 2010), which we call, ISTO; iii) ~~the~~ Moderate Resolution Imaging Spectroradiometer (MODIS) ~~products~~. In comparison to ground based SYNOP measurements, we achieved a promising agreement better than 95 % and 83 % within ± 2 and ± 1 okta respectively. In general, ASCIA shows an improved performance in comparison to other algorithms applied to AATSR measurements for ~~the~~ cloud identification ~~of clouds in a ground scene observed~~ at high latitudes.

1 Introduction

27 The large trends in warming over the Arctic in recent decades, has received much attention from the global and
28 regional climate change research community (Wendisch et al., 2017; Cohen et al., 2014). ~~This study is part of~~
29 ~~research activities to meet the scientific objectives of Collaborative Research Centers, CRC/Transregio 172 “Arctic~~
30 ~~Amplification: Climate Relevant Atmospheric and Surface Processes, and Feedback Mechanisms (AC)³ (Wendisch~~
31 ~~et al., 2017).~~ A number of studies using global observations and climate models confirm this phenomenon, called
32 Arctic Amplification and provide evidence that its impacts extends ~~grows~~ beyond the Arctic (Kim et al., 2017;
33 Cohen et al., 2014). Though, the attribution of the origins of this phenomenon is controversially discussed (Serreze
34 et al., 2011; Pithan et al., 2014), cloud cover is well-known to play a role in the Arctic surface-atmosphere radiation
35 balance (Kellogg et al., 1975; Curry et al., 1996). The accurate identification of Arctic clouds in the ground scenes
36 of remote sensing measurements made from space is therefore of intrinsic importance. However, cloud identification
37 and screening over the Arctic is a challenging task. Since, all developed cloud detection methods encounter many
38 obstacles originating from the unique atmosphere and surface conditions in the Arctic (Curry et al., 1996). The
39 Arctic clouds are mostly optically thin and low with no remarkable contrast in the commonly used visible or thermal
40 or microwave measurements to the underlying surface covered with highly reflecting snow and ice. For example,
41 snow/ice are also like clouds cold, the lack of strong thermal contrast is a limitation in the retrieval of clouds in the
42 thermal infrared (Rossow and Garder 1993; Curry et al., 1996).

43 In addition to the importance of clouds to Arctic Amplification, errors in the identification of cloud within a
44 ground ~~in~~ scene are also one of the major sources of error in retrievals of a variety of data products for both satellite
45 and ground-based measurements at high latitude. For example ~~instance~~, the interference of cloud contamination in
46 the Aerosol Optical Thickness (AOT) retrieved by passive satellite remote sensing is a well-known issue (Shi et al.,
47 2014; Várnai and Marshak, 2015; Christensen et al., 2017; Arola et al., 2017). This limits the reliability and
48 usefulness of the AOT products in the assessment of the direct/ indirect impact of aerosols in Earth’s energy balance
49 in particular over the Arctic. To avoid the uncertainty included in AOT products due to significant misclassification
50 of heavy aerosol load as by thin clouds (which have similar reflectance properties) the development of an adequate
51 cloud identification algorithm is a prerequisite (Martins et al., 2002; Remer et al., 2012; Wind et al., 2016; Mei et al.,
52 2017a, 2017b; Christensen et al., 2017).

53 One recent approach to detect cloud-free snow and ice ~~for aerosol retrieval~~ over high latitudes used the spectral
54 shape of clear snow, ISTO (Istomina et al., 2010). The latter analyses the spectral behavior of each ground scene and
55 identifies clear snow or ice scenes from Advanced Along-Track Scanning Radiometer (AATSR) measurements.
56 Thresholds of the reflectance were empirically determined in seven spectral channels from the VIS to TIR. Defining
57 a reliable threshold which can guarantee a successful separation of cloud and cloud-free regions for the wide range
58 of atmospheric conditions and surface types is a challenging task. This is because of the similarity between spectral
59 reflectance of cloud and snow-ice (Lyapustin et al., 2008). In spite of progress made by this approach, adequate
60 discrimination of thin cloud above ice or snow is an inherent limitation of such threshold based techniques.

61 The European Space Agency (ESA) standard cloud product from AATSR is another example of an existing cloud
62 data product over the Arctic. This operational cloud mask is called the Synthesis of ATSR Data Into Sea-Surface
63 Temperature (SADIST) and is based on the latitudinal thresholds for various cloud types (Ghent et al., 2017). ~~The~~

64 SADIST was initially developed for cloud screening over the ocean (Zavody et al., 2000). Birks et al. (2007)
65 modified this method to apply it over land. Later, Kolmonen et al. (2013) reported that the cloud flags included in
66 AATSR product are noticeably restricted and using this cloud product results in aerosol episodes not being observed.
67 [SADIST is known to misclassify ice, cloud and open ocean in Polar Regions. Bulgin et al. \(2015\) developed a](#)
68 [Bayesian approach in ESA's Climate Change Initiative \(CCI\) project to overcome this limitation \(Hollmann et al.,](#)
69 [2013\).](#) Sobrino et al. (2016) reviewed different cloud clearing methods including the AATSR operational cloud mask
70 in the framework of Synergistic Use of The Sentinel Missions For Estimating And Monitoring Land Surface
71 Temperature (SEN4LST) project. ~~They~~ highlighted the potential uncertainty in different versions of this product,
72 which result in these errors being propagated in subsequent data products. For example, the AATSR operational
73 cloud mask falsely detects cloud in ~ 16 % of the observations. This is attributed to the flagging of land features
74 (such as rivers) incorrectly as cloud (see Sobrino et al., 2013).

75 To avoid the uncertainty arising from the similarity of spectral characteristics of snow, ice and clouds, we decided
76 to develop an algorithm based on a different strategy, namely the use of time series measurements. The use of abrupt
77 changes of TOA reflectance in time with the aim of cloud identification has been reported previously (Gómez-Chova
78 et al., 2017; Lyapustin et al., 2008). An early example of this idea was proposed for low to middle latitudes by
79 Rossow and Garder (1993) in the International Satellite Cloud Climatology Project (ISCCP). This method later
80 evolved as a part of MultiAngle Implementation of Atmospheric Correction (MAIAC) algorithm (Lyapustin et al.,
81 2008), ~~which MAIAC~~ is mainly designed for use with observations over land (low to middle latitudes), where the
82 aim is to simultaneously retrieve aerosol and surface properties. However, it has also been utilized by another study
83 to identify snow grain size over Greenland (Lyapustin et al., 2009). Though, further optimization for the Arctic
84 region is required and reported, a better performance in comparison to Moderate Resolution Imaging
85 Spectroradiometer (MODIS) cloud mask is reported by Lyapustin et al. (2009).

86 The central assumption used in these algorithms for cloud identification, is that clear-sky reflectance is different to
87 that of clouds, which exhibit, [in comparison, a](#) high variation as a function of time (Lyapustin et al., 2008; Gómez-
88 Chova et al., 2017). Knowledge of cloud-free scenes within a given time period, is achieved from knowledge of the
89 variability of the measured TOA reflectance. Covariance analysis is used to estimate the spatial coherence. This has
90 a long history in remote sensing studies using time series measurements (Leese et al., 1970; Lyapustin et al., 2008).
91 The covariance computation assumes changes in the textural patterns of the observed scene, which originate from
92 natural and man-made features such as topography, lakes or urban areas (Lyapustin et al., 2008). The use of the
93 covariance analysis, which accounts for geometrical structures, minimizes issues originating from illumination
94 variation and results in the same algorithm being applicable over both dark and bright surfaces (Lyapustin et al.,
95 2008). For these reasons we decided to use Pearson Correlation Coefficient (PCC) as a function of covariance value
96 for cloud detection over the Arctic. However, Lyapustin et al. (2008) reported that in spite of relative good
97 performance, the covariance itself is not alone adequate for cloud identification in the case of homogenous surfaces
98 or thin clouds. Therefore, we decided to use a combination of a PCC analysis and the reflectance of solar radiation at
99 3.7 μm . The latter utilizes the contrast between cloud and underlying surface making it possible to distinguish cloud-
100 free snow and ice.

101 Another argument in favor of the use of time series analysis is the availability of multiple images by the AATSR
102 and Sea and Land Surface Temperature Radiometer (SLSTR) sensor over the Arctic. For AATSR the revisit time of
103 3-4 days over mid-latitudes (Kolmonen et al., 2016) with more frequent at higher latitude which increase to 2 days
104 over the Arctic (Soliman et al., 2012; Mei et al., 2013). In addition to multiple imagery over the Arctic, the shorter
105 time interval between satellites over-passes over the same scene provides images with less variability in the observed
106 cloud-free areas which the algorithm looks for. For the two SLSTR, the revisit time ~~it~~ is 0.9 days at the equator
107 (Coppo et al., 2010) and this time becomes even shorter at ~~with these values increasing at~~ higher latitudes due to
108 orbital convergence.

109 The AATSR/SLSTR Cloud Identification Algorithm (ASCIA) has been developed as a part of research activities
110 to meet the scientific objectives of Collaborative Research Centers, CRC/Transregio 172 “Arctic Amplification:
111 Climate Relevant Atmospheric and Surface Processes, and Feedback Mechanisms (AC)³ project (Wendisch et al.,
112 2017). ~~for use in the (AC)³ project (Wendisch et al., 2017).~~ The project aims to identify, investigate and evaluate
113 parameters and feedback mechanisms which contribute to Arctic Aamplification (Wendisch et al., 2017).
114 Consequently, a long-term data record of AOT and cloud is required. It is planned to use ~~the~~ ASCIA to identify
115 cloud free scenes for AOT retrieval. It is also planned to ~~be~~ apply itied to the observations acquired by ~~the~~ SLSTR
116 onboard Sentinel-3A and Sentinel-3B launched in 2016 and 2018 respectively which provide continuity of AATSR
117 observations.

118 A full description of ~~the~~ this new cloud identification and its application to AATSR data is presented in the
119 following sections of this manuscript. First, a brief data description is presented in Sect. 2. The theory and
120 methodology, used in our new ASCIA, are discussed in detail in Sect. 3 and 4. We evaluated the performance of ~~the~~
121 ASCIA by comparison of the cloud identification with i) that of the ESA standard cloud product for AATSR level2
122 nadir cloud flag; ii) the data obtained by applying ISTO to AATSR data; while ASCIA is also applied to AATSR
123 nadir observations, those obtained by applying ISTO, iii) the MODIS cloud mask; iv) the Surface synoptic
124 observations (SYNOP); and vi) the AERosol RObotic NETwork (AERONET). The results of the comparisons with
125 these five different ~~source~~ source of cloud data are reported in Sect. 56. A discussion and set of conclusions, drawn
126 from the study, are presented in Sect. 67.

127 2 Instruments and Data

128 2.1 AATSR data

129 The AATSR sensor flown on board polar orbiting Envisat was primarily designed for measuring Sea Surface
130 Temperature (SST) with accuracy higher than 0.3 K. ~~after~~ As the successor of ATSR-1 and ATSR-2 on European
131 Remote Sensing-1, ERS-1 and ERS-2, (<http://envisat.esa.int/handbooks/aatsr/CNTR.html>). ~~The~~ AATSR delivered
132 data from March 2002 until Envisat failed in 2012 (<http://envisat.esa.int/handbooks/aatsr/CNTR.html>). The unique
133 design of spectral coverage of AATSR enabled this sensor to measure reflected and emitted radiances in the VIS,
134 (0.55 μm , 0.66 μm), NIR (0.87 μm , 1.6 μm) and three TIR channels (3.7 μm , 10.85 μm , 12.00 μm) with spatial
135 resolution of $1 \times 1 \text{ km}^2$ at nadir view and swath wide of 512 km. In Fig. 1 one example of the AATSR image over
136 Svalbard is shown. It comprises three different wavelengths to highlight the different information, which are

137 ~~retrieved~~~~one can gain~~ from the wide spectral coverage of this instrument. For example, in ~~the~~ upper right panel ~~of~~
138 Fig. 1 the large ~~change drop of in~~ reflectance over snow/ice created a notable contrast between the cloud and the
139 underlying surface at this wavelength ~~as compared in comparison~~ to that found from the VIS channels used in the
140 R(0.66 μm) G(0.87 μm) B(0.55 μm) image. A similar ~~significant difference~~~~separation~~ of snow/ice and cloud is
141 observed in the reflectance at 3.7 μm shown in the lower left panel in Fig. 1. However, at the longer wavelength of
142 11 μm thin cloud patterns appear in the south-western scenes close to and above Svalbard, which have small
143 signatures in the shorter wavelength. Combining the information from the different channels in an appropriate way
144 enables the presence of cloud in the ground scenes to be accurately identified.

145 The conical imaging geometry of AATSR yields the dual viewing capability of this sensor. Each scene ~~is~~~~was~~
146 imaged twice. The first measurement of the ground scenes is in the forward direction at a viewing angle of 55°. The
147 second occurs 150 sec later at a near-nadir viewing angle. This capability is a design feature of AATSR to deliver an
148 optimal and accurate atmospheric correction and thereby invert an accurate surface reflectance. The two views
149 theoretically yield independent information about atmosphere and the surface to be retrieved.
150 (<http://envisat.esa.int/handbooks/aatsr/CNTR.html>). The dual view approach intrinsically provides more information
151 than the single view for the study of surfaces with complex reflectance characteristics, such as snow and ice
152 (Istomina, 2012).

153 ~~—Examples of AOT algorithms applied to AATSR data are as follows: the AATSR Dual View algorithm (ADV)~~
154 ~~which was initially proposed by Veeffkind et al. (1999) and AATSR single view algorithm (ASV) by Veeffkind et al.~~
155 ~~(1998), the Swansea University (SU) algorithm (North et al., 1999) and Oxford RAL Aerosol and Cloud retrieval~~
156 ~~(ORAC) algorithm (Thomas et al., 2009). These algorithms typically not optimized for the retrieval of AOT at high~~
157 ~~latitudes. As the first task in delivering an algorithm, which delivers AOT at high latitude, ~~t~~The new ASCIA has~~
158 ~~been applied to AATSR measurements~~ to identify cloud and cloud free ground scenes, ~~has been applied to AATSR~~
159 ~~measurements.~~

160 2.2 SLSTR data

161 ~~The~~ SLSTR on-board Sentinel-3A was launched on the 16th ~~of~~ February in 2016 as the successor ~~to~~~~of~~ AATSR ~~series~~
162 to provide the continuity of long term SST measurements. The Sentinel-3B satellite, which contains an identical
163 payload, was also launched by a Rockot/Breeze-KM launch vehicle from the Plesetsk Cosmodrome in northern
164 Russia, on the 25th ~~of~~ April 2018. The design of the SLSTR instrument has some significant improvements with
165 respect to ATSR (Coppo et al., 2010). For example, the swath width of single view and dual view was increased
166 from 500 km to 1420 km and 750 km respectively. This yields global revisit times of 1.9 days at ~~the~~ equator ~~with~~
167 ~~two satellites for the dual view~~ and 0.9 ~~+~~day ~~with one satellite for the single view~~. There are measurements of two
168 additional channels in the SWIR, at the wavelengths of 1.37 μm and 2.25 μm , which are used to provide more
169 accurate cloud, cirrus and aerosol information and used to correct for atmospheric radiative transfer effects in the
170 determination of surface reflectance (Coppo et al., 2010). The Fig. 2 upper right panel shows the use of the new 1.37
171 μm measurements to detect thin cirrus clouds, which are only weakly identified in reflectance at 3.7 μm shown in
172 Fig. 2. ~~The current design of ASCIA does not yet include 1.37 μm measurements. This is because~~As the radiance

173 and TOA reflectance at this wavelength are not measured by AATSR, ~~and because of~~ In addition, SLSTR data at
174 this wavelength currently have unresolved calibration issues. ~~in SLSTR data, the current design of ASCIA does not~~
175 ~~yet include 1.37 μm measurements. In addition, water vapor absorption above and within clouds is considered as an~~
176 ~~obstacle in using this channel for cirrus detection (Meyer et al., 2010).~~ Nevertheless, the use of the measurements at
177 this wavelength in thin cirrus detection should improve the performance of ASCIA in the future. SLSTR also has a
178 higher spatial resolution of $0.5 \times 0.5 \text{ km}^2$ in the VIS and SWIR measurements and two channels dedicated to fire
179 detection (Coppo et al., 2010). The use of the observations from SLSTR and AATSR enables a long-term time
180 series of clouds and aerosol parameters including AOT over the Arctic to be derived. However, there is a ~ 4 years
181 gap between the failure of AATSR and the launch of SLSTR. To fill this gap, we will apply ASCIA also to the
182 Advanced Very High Resolution Radiometer (AVHRR) sensor carried by National Oceanic and Atmospheric
183 Administration (NOAA).

184 2.3 Data used in the cloud identification comparison studies

185 2.3.1 SYNOP

186 The SYNOP have been provided by World Meteorological Organization (WMO) ~~for with~~ the purpose of mapping
187 ~~large-scale~~ weather information around the world. However, the availability of the data is limited in the Arctic
188 ~~studies~~ due to the coverage of SYNOP stations in this region. For example, ~~there are almost~~ almost no
189 ~~observation absent~~ in the central parts of the Arctic Circle as is shown in Fig. 3. The SYNOP measurements, which
190 are made by an observer or, an -automated ~~device fixed stations~~ are available in a standardized layout of numerical
191 code which is called FM-12 by WMO (1995). The SYNOP reports include a variety of meteorological parameters
192 such as temperature, barometric pressure, visibility etc. as well as cloud amount which are observed at synoptic
193 hours simultaneously throughout the globe. We used SYNOP cloud fraction, which have a temporal resolution of 1-
194 3 hours, to evaluate the performance of our new developed ASCIA over the Arctic region.

195 The use of SYNOP measurements to validate a cloud identification algorithm, or for that matter the cloud
196 predicted by a climate model, the fact that the SYNOP cloud fraction is reported using the ~~in~~ okta scale, has to be
197 appropriately taken into account. ~~which ranges from 0 (completely clear sky) to 8 (completely obscured by clouds)~~
198 ~~has to be appropriately taken into account.~~ Converting discrete okta values, which ranges from 0 (completely clear
199 sky) to 8 (completely obscured by clouds) to continuous percentage ones has been done in different ways by
200 climatologists. A common assumption is that 1 okta equals 12.5 % of cloud coverage (Boers et al., 2010; Kotarba,
201 2009). For use in this study it was necessary to make an estimate of the error or uncertainty in the okta in
202 measurements. It is assumed that the man-made nature of cloudiness okta estimation have errors of ± 1 okta and even
203 larger values of ± 2 okta ~~for in~~ the non 0 or 8 okta situations (Boers et al., 2010; Werkmeister et al., 2015). Boers et
204 al. (2010) suggested defining a larger range of 18.75 % for 1 okta instead of commonly used value of 12.5 %. We
205 used this approach and defined percentage of cloud values for each okta, which are given in Table 1. More details
206 about validation procedure are provided in Sect. 6.

207 2.3.2 AERONET

The AERONET is a network of approximately 700 ground-based sun photometers established by National Aeronautics and Space Administration (NASA) and PHOTométrie pour le Traitement Opérationnel de Normalisation Satellitaire (PHOTONS). This globally distributed network aims to provide long-term and continuous measurements of AOT, inversion products and perceptible water in diverse aerosol regimes (Holben et al., 1998). The high temporal resolution of 15 minutes [for these data](#), expected low accuracy of ~ 0.01 to 0.021 (Eck et al., 1999) as well as readily accessible public domain database provides a suitable dataset for aerosol research and characterization.

AERONET data are categorized and available in 3 levels: Level 1.0 (unscreened), Level 1.5 (cloud screened and quality controlled) and level 2.0 (quality assured). The data used in this work are selected from Level 1.5 to validate cloud identification results from newly developed ASCIA. More details of validation procedure are discussed in Sect. 6.

3 Theoretical background

3.1 Pearson Correlation Coefficient (PCC)

The PCC was proposed by Karl Pearson (1896) and is used in this study as an indicator of the correlation between sequential AATSR measurements. The PCC is also known as the Pearson Product-Moment Correlation Coefficient (PPMCC). It is a standard dimensionless statistical parameter commonly used to measure the strength and direction of the linear association between a pair of variables (Benesty et al., 2009). This parameter has extensively been used in many studies which pursue pattern analysis and recognition.

Our ~~use of the~~ PCC analysis ~~is to~~ separates the surface reflectance at a given viewing angle, which is stable over short time periods, from the cloud reflectance, which is highly variable over [a](#) short time period. To describe the computational procedure developed [here](#), ~~we let~~ assume x , y ~~to be as~~ two random variables, then [the](#) PCC can be written as a function of [the](#) covariance of x and y which is normalized by square root of their variances (Rodgers et al., 1988; Benesty et al., 2009):

$$PCC = \frac{COV(x, y)}{\sigma_x \sigma_y}, \quad (1)$$

where $COV(x, y)$ is the covariance of variables and σ is the root-mean-square variations of each random variables (Rodgers et al., 1988; Benesty et al., 2009):

$$COV(x, y) = \frac{1}{N^2} \sum \sum (x_i - \bar{x})(y_i - \bar{y}) \text{ and } \sigma_x^2 = \frac{1}{N^2} \sum_{i=1}^N (x_i - \bar{x})^2, \quad (2)$$

$$PCC = \frac{\sum (x_i - \bar{x})(y_i - \bar{y})}{(\sum (x_i - \bar{x})^2 \sum (y_i - \bar{y})^2)^{1/2}}, \quad (3)$$

where \bar{x} and \bar{y} are the mean value of x and y variables respectively. The correlation coefficient parameter has values between -1 and +1 (Rodgers et al., 1988). The PCC values were prepared in this study. The association between the two variables is stronger if the absolute value is closer to 1, whereas if two variables are independent or in another

word “uncorrelated” PCC value will become 0 (Benesty et al., 2009). As a consequence of the above the PCC values computed between several data pairs for ground scenes of the same area at different times provide an indication of whether the scene is cloud covered or free of clouds.

For this aim, the use of all seven channels (0.55 μm , 0.66 μm , 0.87 μm , 1.6 μm , 3.7 μm , 11 and 12 μm) was investigated. The visible channels (0.55 μm , 0.66 μm) on their own are not optimal to separate cloud free from cloudy scenes, in particular for thin clouds. The SWIR and TIR such as 1.6 μm and beyond, where liquid water and ice absorb provide useful information. There is a large reduction of reflectance between clear snow/ice as compared to clouds between 0.87 μm and 1.6 μm (Kokhanovsky, 2006). Our routine takes advantage of this contrast through the PCC calculation. ~~One major contributors of error in aerosol retrieval is misclassifying heavy aerosol loads with clouds.~~ One of the major contributors to error in aerosol retrievals is misclassification of heavy aerosol loads as cloud. Using 1.6 μm reflectance which is less affected by aerosols than visible wavelengths addresses in part this issue (Lyapustin et al., 2008).

A second question in PCC analysis (after wavelength selection) is definition of the optimal size of the block of ground scene for PCC calculation. In early version of current algorithm, we set up 10 \times 10 km² as the block size. Since, aerosol retrieval would be carry out with the same spatial resolution. However, our investigations and previous studies show that 10 \times 10 km² is not sufficient to capture surface patterns. Thus, blocks of 25 \times 25 km² area as proposed in previous studies (Lyapustin et al., 2008) were used. The implementation of PCC analysis as used in this study is discussed in more detail in Sect. 4.

3.2 Reflectance of 3.7 μm thermal infrared channel

The reflectance part of TIR Channels at 3.7 μm and 3.9 μm have been used in different studies to determine cloud properties such as cloud effective radius and thermodynamic phase of the cloud or to discriminate cloud and snow/ice covered surface (Meirink et al., 2016; Klüser et al., 2015; Musial et al., 2014; Khlopenkov, et al., 2007; Pavolonis et al., 2005; Rosenfeld et al., 2004; Spangenberg et al., 2001; Allen et al., 1990). The reason for the wide application of this channel in cloud identification methods is the difference in Single Scattering Albedo (SSA) at this band compared to shorter VIS and INR wavelengths, which in turn results from the significant sensitivity of SSA to thermodynamic phase and particle size of clouds (Platnick et al., 2008). For example, the scattering of liquid clouds, having small droplets, is relatively larger than absorption and the ratio of NIR/VIS reflectance approaches 1. ~~But~~ while in the case of large liquid droplets or ice particles, the absorption increases and this ratio is closer to zero (Platnick et al., 2008).

~~—~~In addition, cloud-free snow reflects at a relatively weak level in comparison to clouds at 3.7 μm channel (Derrien et al., 1993; Platnick et al., 2008). Therefore, the contrast due to different physical properties and radiance of snow/ice and cloud at 3.7 μm makes the use of this channel advantageous for the identification of clouds. During daytime, the measured Brightness Temperature (BT) at 3.7 μm is determined from the upwelling radiation which comprises both reflected or scattered solar radiation and the thermal emission from the surface (Musial et al., 2014). To use TOA reflectance at 3.7 μm , procedures are needed to account for and subtract the emission portion of measured BT at 3.7 μm wavelength (Allen et al., 1990). To achieve this goal independent information about the

271 surface TIR is needed. This is estimated from observations at 11 μm where absorption by water vapor and other
 272 trace gases is ~~very small~~; most ~~objects-phenomena in regions outside of the tropics can be treated~~ behave as
 273 blackbodies and the measured BT considered ~~being in good agreement with as-the~~ real surface temperature
 274 (Istomina et al., 2010; Musial et al., 2014).

275 To do that, we use the method described in Meirink et al. (2016) and Musial et al. (2014), where the reflectance of
 276 3.7 μm can be written as:

$$R_{3.7} = \frac{L_{3.7} - B_{3.7}(T_{11})}{\mu_0 F_{3.7,0} - B_{3.7}(T_{11})}, \quad (4)$$

277 where $R_{3.7}$ is the reflectance i.e. the ratio of scattered radiance to incident solar radiance; $L_{3.7}$ is measured radiance at
 278 3.7 μm ; $B_{3.7}(T_{11})$ ~~the Planck function radiance (the contribution from thermal emission at 3.7 μm) is the Planck~~
 279 ~~function radiance $B_{3.7}(T_{11})$ estimated from the temperature value obtained from the T_{11} measurements at 11 μm ;~~
 280 $F_{3.7,0}$ is the solar constant at 3.7 μm ~~and which is weighted by μ_0 as~~ the cosine of solar zenith angle.

281 Theoretical reflectance values at 3.7 μm band, computed by Allen et al. (1990) have been compared to satellite
 282 measurements at the same channel from Advanced Very High Resolution Radiometer (AVHRR). The results of this
 283 work are summarized in Table 2. According to this study, the reflectance of liquid clouds primarily depends on
 284 droplet size and solar zenith angle, whereas for ice clouds, ice particle shape and size distribution are of great
 285 importance together with Cloud Optical Thickness (COT) and sun-satellite geometry. The observed reflectance is
 286 reported in a range of 0.08 to 0.36 for liquid clouds and 0.02 to 0.27 for ice clouds (Allen et al., 1990). Arking and
 287 Childs (1985) calculated 3.7 μm reflectance for ice clouds which varies between 0.01 to 0.30 for the COT of 0.1 to
 288 100 and ice crystal effective radius of 2 μm to 32 μm , solar zenith angle of 60°. Spangenberg et al. (2001) reported a
 289 typical value of 0.04 to 0.4 for clouds. In the case of snow covered surface 3.7 μm reflectance is dependent on many
 290 factors including snow grain size, solar zenith angle, liquid water content, snow impurities and etc. Considering the
 291 snow grain size of 50 μm to 200 μm , with a solar zenith angle of 40° to 80°, the modeled values for snow reflectance
 292 varies between 0.005 and 0.025 at 3.7 μm (Allen et al., 1990). However, a range of 0.02 to 0.04 is observed from the
 293 satellite measurements over the same wavelength for snow cover. This difference between model calculations and
 294 measurements is explained by snow impurities (Allen et al., 1990). For land areas, the 3.7 μm reflectance is
 295 impacted by soil type, vegetation type, coverage and moisture content. An average value of 0.15 is derived for clear
 296 sky land scenes at 3.7 μm (Allen et al., 1990). In order to use the remarkable contrast between snow cover and
 297 clouds at 3.7 μm channel, two main issues have to be taken into account: 1) the interference between snow and ice-
 298 cloud values; 2) the interference between cloud and land reflectance. The latter is easily solved by using information
 299 from visible channels with 3.7 μm reflectance. This is because land scenes in Polar region are dark in comparison to
 300 cloud and snow. The first issue, discriminating ice clouds from snow is a challenging task. To detect ice clouds, we
 301 combined 3.7 μm reflectance with PCC analysis. A full description of this new method is given in Sect. 4.

302 4 Methodology

303 The ASCIA implementation is initiated by preparing a time series of data. A time span of one month for the ground
304 scene was selected. Hagolle et al. (2015) indicated that in Sentinel-2 measurements with revisit time of 5 days, most
305 of the given scenes would be observed cloud-free at least once a month. Consequently, we also assume that every
306 scene of AATSR measurements, which have a higher revisit time of 3 days, will be cloud-free at least once a month.

307 Depending on the latitude and the time of year the number of downloaded data varies from 10 to 50 or more over
308 the same scene. AATSR provides more data over higher latitudes, which increase in spring and summer ~~time~~ due to
309 longer polar days and solar illumination. The AATSR L1b data are already provided as gridded and calibrated 1×1
310 km^2 scenes, ~~which~~ These include geo-location information interpolated from the tie point scenes which are equally
311 distributed across a single AATSR image (<http://envisat.esa.int/handbooks/aatsr/CNTR.html>).
312 ~~Consequently~~Therefore, there is no necessity to re-grid them for ~~the~~ geo-referencing step, ~~which~~ This is considered
313 as an advantage, ~~because it~~ ~~to~~ preserves the original reflectance value of each scene for following steps. However,
314 the time series data are acquired by the satellite from different viewing geometries. To compute PCC values over the
315 same areas from different days, the ASCIA ~~selects~~looks for the closest similar scenes using geo-location information
316 provided in the data. The closest distance is often found to be within 0.006 degree and increases to 0.01 degree in
317 the worst case and thus ~~is considered to be~~ of negligible significance. After ~~this procedure to select the~~
318 ~~observations~~finding the same blocks over different dates and building blocks, ~~the~~ ASCIA comprises two main parts
319 ~~to identify the presence of cloud~~: i) a PCC analysis at $1.6 \mu\text{m}$; ii) ~~the use of thresholds for~~Applying thresholds on
320 reflectance of $3.7 \mu\text{m}$ channel.

321 In the first step, a PCC analysis for a block of ground scenes ($25 \times 25 \text{ km}^2$) is used to identify cloud and cloud-free
322 blocks, which are assumed to have low and high PCC values respectively. The output of this step is a binary flag at
323 the block level. This serves as input for the second step to produce at ground scene level ($1 \times 1 \text{ km}^2$ or $0.5 \times 0.5 \text{ km}^2$
324 depending on spatial resolution of instrument) cloud identification, by using the knowledge of the reflectance of
325 solar radiation at $3.7 \mu\text{m}$ channel. The combination of these two constraints is necessary because neither PCC
326 analysis nor reflectance part of $3.7 \mu\text{m}$ channel is adequate on its own for accurate cloud detection. A high PCC
327 value cannot guarantee the clearness of the whole block of scenes (Lyapustin et al., 2008) because some ground
328 scenes may still contain clouds, which are not enough in number to decrease significantly the PCC value. This case
329 occurs frequently over small or semitransparent clouds where the textural pattern of surface is still observable
330 through the clouds (Lyapustin et al., 2008). Small PCC values may be caused by ~~a~~ rapid surface change, ~~or~~ high
331 aerosol load or ~~the~~ lack of recognizable spatial pattern, which is often the case over homogenous snow covered
332 surface (Lyapustin et al., 2008). A PCC value of 0.63 is suggested by Lyapustin et al. (2008) to separate cloud-free
333 blocks over middle latitudes. Considering less surface patterns in a large area of the Arctic compared to lower
334 latitudes, and our PCC analysis over both middle and high latitudes, we defined a lower threshold ~~for~~ PCC of 0.4
335 over the Arctic region and found ~~that~~ ~~the~~ PCC of 0.6 is appropriate for middle latitudes based on ~~a~~ large number of
336 statistical analyses.

337 After computing the first binary cloud flag at block level using ~~the~~ last measurement and one previous image, ~~the~~
338 ASCIA keeps the result in ~~a~~ memory and repeats the procedure with second previous data. ~~This procedure is iterated~~
339 ~~and so on~~, until the last measurement of the data series is involved ~~in PCC analysis~~. The final binary blocks are

340 imported through the second step to identify cloudy scenes based on thresholds defined for blocks with low and high
341 PCC value differently. ~~We note~~ However, we would like to underline that, the snow/ice reflectance at 3.7 μ m
342 channel (~ 0.005 - 0.025) has interference with those of ice clouds (0.01 - 0.3) at this wavelength. To avoid the
343 uncertainty arising from this problem we defined the PCC analysis as a decision point of ASCIA requiring further
344 optimized analysis:

- 345 (i) For the high $PCC \geq 0.4$, the whole block is considered to be cloud free and then ~~the~~ ASCIA starts looking for
346 remaining small cloud scenes within a block, ~~i.e.~~ scenes with $R_{3.7}$ larger than the maximum value observed
347 over snow at 3.7 μ m: $R_{3.7} > 0.04$, (Allen et al., 1990).
- 348 (ii) For $PCC < 0.4$, the block is assumed to be cloudy; ASCIA removes all scenes within the block and only keeps
349 scenes which satisfy the $R_{3.7} < 0.015$ test. This threshold is equal or lower than the lowest observation of ice
350 cloud reflectance at 3.7 μ m (Allen et al., 1990).

351 In our method, PCC analysis constrains the procedure and ~~the~~ strict decision is only made within low PCC blocks.
352 The loss of some clear scenes in low PCC blocks is an unavoidable side effect of using ~~this~~ strict criteria in
353 particular over land scenes, having low PCC and high 3.7 μ m reflectance values. However, ~~the~~ ASCIA detects the
354 presence of thin cirrus cases with a relatively high confidence level. A schematic flowchart of ~~the~~ ASCIA is shown
355 in Fig. 4, with the use of the two main constraints being highlighted. In addition to picking out clear scenes, a simple
356 land classification procedure is undertaken in this step of ~~the~~ ASCIA. Snow/ice scenes are identified with low 3.7
357 μ m reflection whereas land scenes with high reflection are classified with the aid of the darkness test over visible
358 channels. The corresponding thresholds for land classification scheme are described in the Table 3.

359 ~~It is important to note that if one scene, a~~ Although characterized as land, ~~a scene~~ may include soil, different types
360 of vegetation cover or even melting snow. The latter mix with soil and becomes ~~s~~ dark enough to be filtered out from
361 the snow class. Sea-ice is distinguished from water on the basis of its ~~greater~~ ~~higher~~ brightness; one scene might be
362 white enough to be considered as ice. However, melting or broken ice ~~as well as new ice~~ would not be labeled as ice.
363 Snow over sea-ice is not distinguished from pure sea-ice and both of them are labeled as sea-ice. This also means
364 that ice over land is also marked as snow as well as pure snow.

365 A representative examples of the block level (25×25 km²) and scene level (1×1 km²) results of ~~the~~ ASCIA
366 ~~applied to~~ AATSR observations ~~is shown in Fig. 5. This example was selected to show the performance of~~
367 ~~ASCIA in presence of different surface conditions: 1) one scene is over a combination of fairly homogenous snow~~
368 ~~cover, land, ocean, sea-ice and cloud scene at north-west of Greenland taken on the 18 May 2008; 2) another~~
369 ~~example is over a surface with highly variable topography over Svalbard with relatively higher solar zenith angle~~
370 ~~(> 80°) on the 1 March 2008. on the scenes within the region over northwest of Greenland in spring time enclosed in~~
371 ~~the coordinates for four corners (75° N, 48° W), (75° N, 75° W), (81° N, 48° W), (81° N, 75° W) taken on the 18 May~~
372 ~~2008 are shown in Fig. 5. This example selected to show the performance of ASCIA over a combination of fairly~~
373 ~~homogenous snow cover, land, ocean, sea-ice and cloud.~~ As we discussed earlier, the ambiguity of the PCC analysis
374 over homogeneous surfaces on the right ~~and left~~ sides of ~~the~~ AATSR scene in ~~middle panel of~~ Fig. 5, is ~~entirely~~
375 compensated ~~in the right panel~~ by using additional information from 3.7 μ m channel. ~~Another example over a~~
376 ~~surface with highly variable topography in March with relatively higher solar zenith angle (> 80°) is selected over~~

Svalbard enclosed in the coordinates for four corners (75°N, 4°E), (75°N, 32°E), (81°N, 4°E), (81°N, 32°E) taken on the 1 March 2008.

5 Results and validation

5.1 The comparison of ASCIA products with products from other algorithms using space-borne observation

In this study, we applied our recently developed ASCIA to identify cloud in the scenes using AATSR L1b (TOA reflectance) and SLSTR L1b gridded data. The input file to the process chain is one scene of AATSR L1b product the output comprises 5 classes of surface types including snow/ice, sea ice, water, cloud and land. The procedure of surface classification is explained in Sect. 4. The location and time of selected case studies are used to show that the identification of cloud by our new ASCIA is adequate. ~~In this regard,~~ The AATSR data are selected from several years starting from 2006, during strong Arctic haze episode, which originated predominantly from agricultural fires burning in Eastern Europe. The event has been reported in previously (Law et al., 2007). A second episode in 2008 is also considered for which validation data are available from SYNOP stations. ~~Three~~ One months of data from ~~the targeted seasons spring, summer and autumn vis.~~ March, May, and July ~~respectively~~ have been acquired over Greenland and Svalbard to assess the performance of ~~the~~ ASCIA in a wide range of solar zenith angles (60°-85°), surface and atmospheric conditions observed at high latitudes. In order to ~~take take into account~~ various surface types in the Arctic into account, we selected case studies including, highly variable topography and fairly homogenous snow cover, coast lines, land and ocean along snow and ice covered surface. The designed criteria for ~~the~~ ASCIA are optimized for ~~an over~~ various regions ~~over of~~ the Arctic observed under in different solar illumination conditions. Polar night and transition seasons at low light conditions are excluded from our retrievals. ~~with the exception of the dark winter period.~~ The results obtained are compared with i) the AATSR L2 nadir cloud flag and ii) those results obtained with ISTO (Istomina et al., 2010) and iii) MODIS.

As we discussed in Sect. 1, misclassification ~~fying of~~ thin cirrus cloud with clear snow is reported to be ~~as~~ an unresolved problem of ISTO approach. Two representative scenarios of this problem are illustrated in Fig. 6 and Fig. 7 over Greenland and Svalbard respectively in which thin cloud is detected as clear snow by the ISTO method whereas ASCIA confirmed the presence of cloud. ~~In fact,~~ Over such a homogenous surface such as ~~like~~ Greenland, the second step of ~~the~~ ASCIA is decisive ~~plays the main rule.~~ ~~Since,~~ ~~†~~ The lack of structural patterns on surface lead to low PCC values in the first step and consequently overestimation of cloudy scenes. However, the reflection part of 3.7 μm could help to label and bring back clear homogenous surface as cloud free snow in second step. The right panel in Fig. 6 and 7 shows the difference between the result of ASCIA and ISTO. In this panel, the dark blue scenes show clouds, which are not detected by ISTO but are by ~~while~~ the ASCIA could identify them sufficiently. ~~The~~ On the other hand, reddish scenes show cloud free cases, scenes which ISTO failed to detect, ~~them~~ but are correctly labeled by ~~the~~ ASCIA ~~labeled them~~ as cloud free. ~~As we can see,~~ ~~†~~ In addition to the edge of clouds which are difficult to detect ~~specially~~ over snow and ice, there are ~~we have~~ a significant ~~remarkable~~ number of undetected cloud scenes in ISTO results which are identified successfully by ~~the~~ ASCIA. However, for the rest of these two scenes, ~~the both of~~ two algorithms show good ~~a promising~~ agreement.

412 The ESA cloud product from L2 data, ~~shows a significant overestimation of clouds~~ which leads to a loss of
413 ~~missing~~ clear snow and ice scenes. The tendency of this product to flag clear scenes as cloud is also visible in Fig. 6,
414 7. The results in Fig. 8 show undetected clouds as another problem of AATSR level 2 cloud product, which happens
415 frequently ~~at high solar zenith angle~~ winter time. To have a better understanding of this misclassification, we
416 validated the AATSR L2 nadir cloud flag against SYNOP measurements and results are described in Sect. 6.

417 ~~Poor~~ The lack of good performance ~~for in cases~~ winter time over the Arctic with high solar zenith is observed in all
418 of the results using ISTO method. Figure 8 is an example over Svalbard in March 2008. Over such a highly variable
419 surface type, ~~such as like~~ Svalbard, the reflection ~~at part of~~ 3.7 μm ~~can~~ could approach the highest values such as
420 0.035, which is similar to that from cloud reflection. In this ~~difficult~~ case, PCC analysis is of great importance to
421 keep cloud free snow scenes from the strict criteria of second step in particular in ~~cases~~ winter time with higher solar
422 zenith angle. ~~The~~ ASCIA in high PCC block ~~covers~~ accounts a wide range of solar zenith angle (40-80 degree) and
423 results in the reflectance of snow/ice being defined as between 0.02 and 0.04 at 3.7 μm channel. On the right panel
424 ~~of Fig. 8, a relatively one can see the~~ large number of red scenes, which are falsely detected as cloud ~~by in~~ the ISTO
425 method, are observed.

426 Figure 10 shows one example of a haze event over Svalbard on 3rd of May, 2006. Both ~~the of~~ ESA and ISTO
427 cloud products ~~showed~~ had good ~~results~~ performance for this case with the exception of ~~the undetected~~ thin cloud
428 scenes which are falsely ~~labeled~~ detected as clear snow by ~~the~~ ISTO. ~~In fact, t~~ The appropriate design and application
429 of PCC analysis over 1.6 μm enables cloud to be discriminated from heavy aerosol load. However, aerosol load over
430 cloud could not be separated from cloudy scenes.

431 The only season, in which all three approaches detected clouds with similar success, was summer in July as
432 shown in Fig. 9. Although ASCIA shows an overall better performance in particular for thin clouds, the required
433 computational time for cloud detection and surface classification is higher than two other methods.

434 ~~In addition, w~~ We also compared our results with those from the MODIS cloud identification algorithm used for
435 masking cloudy ~~ed~~ scenes. As an example, Fig. 11 shows the AATSR scene over Svalbard on 14th July 2008, where
436 a large part of sea-ice is covered with thin clouds which have a small signature in visible channels. The middle panel
437 shows the MODIS cloud mask for the same area. Although there is a small time difference of 15 minutes between
438 MODIS and AATSR overpasses, we see that scenes identified ~~as with~~ cloudy by ASCIA correspond well with those
439 of MODIS.

440 Figure 12 shows another example over northwest of Greenland on 18th May 2008. The thin and broken clouds are
441 well detected over the snow cover by ASCIA, as well as the clouds over the southern part of the scene, which is
442 covered with snow and ocean. As we can see from the comparison between ASCIA and MODIS cloud scene
443 identification, cloudy scenes in the northern part of scene are not captured by MODIS product but the presence of
444 clouds is seen in the RGB image in left panel. We observed other cases with similar differences especially for the
445 case of thin and broken clouds. There are two potential sources of these differences, 1) time differences, which are
446 10 minutes in this case, or 2) ~~an inadequate~~ proper performance of the MODIS cloud mask over bright surfaces
447 covered by snow and ice.

448 Due to the loss of Envisat and thus AATSR data in 2012, and the need for long time series of [consistent](#) data, we
449 tested ASCIA on the AATSR successor SLSTR as well. Figure 13 shows some results over Svalbard on the 18th [of](#)
450 April 2017. Due to the smaller swath width of AATSR compared to SLSTR, ~~the~~ ASCIA is not applied to the full
451 coverage of SLSTR and the selected scene is cropped to have ~~a~~ similar coverage of 500×500 km². In spite of
452 some unresolved calibration issues in this sensor, the higher spatial resolution in SLSTR clearly helps to improve
453 cloud identification in first step, because the PCC analysis is more sensitive to smaller changes in 0.5×0.5 km²
454 scenes, [as](#) compared to 1×1 km². Moreover, the shorter revisit time of the Sentinel-3 satellite provides more acquired
455 images over the same scene. This results in a larger number of reference images, compared to those from Envisat.
456 Overall these effects result in ~~the ASCIA~~ [an expected improved performance of ASCIA when applied to application](#)
457 ~~on SLSTR data being improved to the performance with, as compared to when applied to AATSR. However, t~~ The
458 comparison of MODIS and ASCIA results indicates that ASCIA detected more cloudy scenes than the MODIS
459 algorithm [in agreement with the above](#).

460 [5.2 The comparison to ground-based measurements: SYNOP and AERONET](#)

461 ~~6—Validation~~

462 In this section, we present a quantitative validation of our ASCIA results by making comparisons with simultaneous
463 ground-based SYNOP and AERONET measurements. The ESA standard cloud product is also compared with these
464 validation data sets. The difference in spatial and temporal resolution of the new cloud identification datasets and the
465 data sets used to validate this dataset has to be taken into account. [To define the optimal maximum temporal](#)
466 [difference between SYNOP and satellite data, other comparable validation activities used different temporal](#)
467 [intervals like 10 min \(Werkmeister et al., 2015\), 15 min \(Musial et al., 2014\), 1 h \(Dybbroe et al., 2005\) and 4 h](#)
468 [\(Meerkötter et al., 2004\). The investigation and results in the previous publications indicate that temporal difference](#)
469 [in validation of satellite retrievals against SYNOP depend on meteorological conditions. Allowing only a small](#)
470 [temporal difference between measurement datasets \(here: SYNOP and ASCIA\) ensures an optimal temporal overall](#)
471 [but can introduce a significant sampling error due to the small number of scenes for validation \(Bojanowski et al.,](#)
472 [2014\). According to Bojanowski et al. \(2014\) a temporal difference of 90 min to compare with SYNOP](#)
473 [measurements at temporal resolution of 3 h minimizes the sampling error \(Bojanowski et al., 2014\). However,](#)
474 [potential longer temporal difference will introduce an error which should be considered along other sources of](#)
475 [uncertainty \(different viewing perspective, different spatial footprint and etc.\). In this study, the maximum allowed](#)
476 [temporal difference between the ASCIA retrievals and SYNOP measurements is less than ±20 minutes in most cases](#)
477 [and generally does not exceed ± 45 minutes.](#) ~~The difference in the time of satellite and SYNOP measurements is~~
478 ~~small being below ±20 minutes in most cases and generally does not exceed ± 45 minutes.~~ To compare surface
479 measurement from SYNOP hemispheric view with the cloud identification at a spatial resolution 1×1 km² resolution
480 satellite measurement, we calculated cloudiness as the percentage of cloudy scenes within a window of 20×20 km²
481 around each SYNOP station. This is a similar distance to that used in previous studies to validate satellite based
482 cloud identification SYNOP or similar surface measurements (Kotarba, 2017; Werkmeister et al., 2015; Minnis et

al., 2003). The cloud detection data product was then compared to the three selected months (March, May and July) of SYNOP observations. These result in~~comprise~~ 100 measurements over Svalbard and Greenland.

In Fig. 14 we present the relation between the calculated Cloud Fractional Cover (CFC) from ASCIA and SYNOP measurements and density plot of occurrences of the CFC by ASCIA as a function of SYNOP following the idea of Werkmeister et al. (2015). ~~The~~We find that these two data sets have a correlation coefficient of $R=0.92$. In 31 % of scenarios, ASCIA estimates 1 okta more than SYNOP while in 14 % of match-ups SYNOP shows higher CFC of 1 okta. Figure 14 also reveals that most of ± 1 okta differences occur when either SYNOP or ASCIA estimates 7 or 8 oktas which could be due to definition of 8 oktas (100 % CFC) and conversion of continuous percentage to okta (Werkmeister et al., 2015). For instance, CFC of 99.9 % is considered as 7 oktas by using Table 1, but~~while~~ the CFC difference is only 0.1 % with 8 oktas. The underestimation of CFC by SYNOP is also indicated~~confirmed~~ in the histogram of difference between ASCIA-SYNOP in Fig. 15. ~~This underestimation-~~ which was confirmed~~indicated~~ by~~in~~ previous studies as well (Kotarba, 2009; Werkmeister et al., 2015). We also indicate the higher accuracy of ASCIA for cloud detection compared to the ESA cloud product. The results of the validation are summarized in Table 4. The cloud cover reported from SYNOP agrees in~~has an overall agreement of~~ 96 % (within ± 2 okta) and 83 % (within ± 1 okta) of the observations with the cloud identification data from ASCIA. As ~~we~~ discussed earlier an error of ± 1 to ± 2 okta would be expected as the accepted accuracy range from~~form~~ SYNOP cloud cover values due to man-made nature of its observation and viewing conditions (Boers et al., 2010; Werkmeister et al., 2015). In comparison, ~~T~~he ESA cloud product agrees 68 % (within ± 2 okta) and 50 % (within ± 1 okta) with SYNOP CFCs. The larger differences of SYNOP and ESA cloud product are also indicated in Fig. 16 where the CFC values in percentage are shown for ASCIA, ESA and SYNOP for validation scenarios. The blue error bars, indicate the range of okta values for each SYNOP as explained in~~according to~~ Table 1.

We also validated ASCIA cloud identification results with AERONET level 1.5 measurements, which ~~are~~ cloud screened. The procedure for this validation takes place in 2 steps: (1) covering AERONET observed AOT to a cloud flag (AOT is provided in AERONET only in cloud-free conditions); (2) Validation of ASCIA with AERONET cloud flag. ~~In~~ 86.1 % of 36 studied~~s~~ scenes over Svalbard, both ASCIA and AERONET confirm the presence of clouds.

6.7 Conclusions

A new cloud detection algorithm, called ASCIA, for use at high altitudes above bright surfaces has been developed to generate stand-alone products and for subsequent use in the retrieval of AOT over the Arctic. ASCIA has been developed for use with the~~uses~~ data from the European instruments ~~using~~-AATSR on the ESA Envisat (2002 to 2012) and SLSTR on the ESA Sentinel 3A or 3B. ~~The~~ ASCIA employs initially a time series analysis of PCC to identify cloud presence, the stability and cloud-free conditions at the block scale of scenes ($25 \times 25 \text{ km}^2$). It then uses the $3.7 \text{ }\mu\text{m}$ solar reflectance to discriminate cloud presence at the spatial resolution of the scene ~~level~~, which is $1 \times 1 \text{ km}^2$ or $0.5 \times 0.5 \text{ km}^2$ for AATSR and SLSTR measurements respectively. The PCC parameter analysis of a block of data is independent to a first approximation of threshold settings, which often lead to misclassification of cloud and snow due to the similarity of their spectral characteristics and thus the thresholds. The brightness temperature

519 | measurements from 3.7 μm channel provide [the](#) information to convert a block level [resolution](#) ($25 \times 25 \text{ km}^2$) to a
520 | scene level [resolution](#) ($1 \times 1 \text{ km}^2$ or $0.5 \times 0.5 \text{ km}^2$) cloud identification. ASCIA thereby exploits the contrast in
521 | reflectance between snow/ice and cloud at 3.7 μm wavelength.

522 | The results of applying the new developed ASCIA are compared and validated against 5 existing products and
523 | methods over the Arctic: 1) SYNOP measurements, 2) AERONET measurements, 3) one of existing methods based
524 | on spectral shape of clear snow 4) AATSR L2 nadir cloud flag, 5) MODIS cloud product. The validation ~~is~~ resulted
525 | in overall agreement of 96 % (within ± 2 oktas) and 83 % (within ± 1 okta) between SYNOP and ASCIA. The
526 | comparison of the ASCIA and ISTO methods shows [the improved](#) ~~a better~~ performance of ASCIA in extreme
527 | situations, such as high solar zenith angle conditions.

528 | The validation results indicate that the current ESA AATSR L2 nadir cloud flag often falsely identify clouds over
529 | snow/ice, ~~with the~~ [except](#) ~~ion of~~ during summer. The comparison between [the](#) ESA AATSR L2 cloud product and
530 | SYNOP measurements resulted in [agreement of](#) 68 % (within ± 2 oktas) and 50 % (within ± 1 okta). The overall
531 | better performance of ASCIA has also been [demonstrated](#) ~~shown~~ [when it is applied to](#) ~~by~~ the SLSTR data.
532 | [Nevertheless](#) ~~However, more investigation and an~~ optimization [is](#) ~~are~~ needed for the detection of cloud over land
533 | (soil, vegetation etc.) ~~for~~ in the PCC blocks [having](#) ~~with~~ lower values. [This is because](#) ~~Since,~~ the strict performance of
534 | ~~the~~ ASCIA in cloudy blocks results in scenes of clear land (without snow cover) being identified as cloud due to
535 | high reflectance of land scenes at 3.7 μm channel. [We also note that](#) ~~Additionally,~~ sub-scene cloud detection has not
536 | been studied with the current version of ASCIA. The use of reflectance in the 1.37 μm channel will be tested in the
537 | future to improve thin cirrus detection in ASCIA. [The objective of this study was to assess and validate the current](#)
538 | [version of ASCIA for daytime observations. For night time application, an adaption of ASCIA is planned to identify](#)
539 | [clouds during night.](#)

540 | *Acknowledgements: We gratefully acknowledge the support by the Collaborative Research Centres,*
541 | *CRC/Transregio 172 “Arctic Amplification: Climate Relevant Atmospheric and SurfaCe Processes, and Feedback*
542 | *Mechanisms (AC)³. This work has been funded in part by the DFG CRC 172 and the State and University of*
543 | *Bremen.*

544 | **References**

- 545 | Allen, R. C., Durkee, P. A., and Wash, C. H.: Snow/cloud discrimination with multispectral satellite measurements,
546 | J. Appl. Meteor., 29, 994–1004, 1990.
- 547 | Arking, A. and Childs, J. D.: Retrieval of cloud cover parameters from multispectral satellites images, J. Climate
548 | Appl. Meteor., 24, 322-333, 1985.
- 549 | Arola, A., Eck, T. F., Kokkola, H., Pitkanen, M. R. A., Romakkaniemi, S.: Assessment of cloud-related fine-mode
550 | AOD enhancement based on AERONET SDA product, Atmos. Chem. Phys., 17, 5991–6001, 2017.
- 551 | Benesty, J., Chen, J., Huang, Y., Cohen, I.: Noise Reduction in Speech Processing, Springer Topics in Signal
552 | Processing 2, Springer-Verlag Berlin Heidelberg, doi: 10.1007/978-3-642-00296-0_5, 2009.

553 Birks, A. R.: Improvements to the AATSR IPF relating to Land Surface Temperature Retrieval and Cloud Clearing
554 over Land, AATSR Technical Note, Rutherford Appleton Laboratory, Chilton, UK, 2007.

555 Boers R., de Haij, M.J., Wauben, W. M. F., Baltink, H. K., van Ulft, L. H., Savenije, M., Long, C. N.: Optimized
556 fractional cloudiness determination from five ground-based remote sensing techniques, *J. Geophys. Res.*, 115,
557 D24116, 2010.

558 [Bojanowski, J., Stöckli, R., Tetzlaff, A., and Kunz, H.: The Impact of Time Difference between Satellite Overpass
559 and Ground Observation on Cloud Cover Performance Statistics, *Remote Sensing*, 6, 12 866–12 884,
560 <https://doi.org/10.3390/rs61212866>, 2014.](#)

561 [Bulgin, C. E., Eastwood, S., Embury, O., Merchant, C. J. and Donlon, C., Sea surface temperature climate change
562 initiative: alternative image classification algorithms for sea-ice affected oceans. *Remote Sens. Environ.*, 162, pp.
563 396-407, 2015.](#)

564 Christensen, M. W., Neubauer, D., Poulsen, C. A., Thomas, G. E., McGarragh, G. R., Povey, A. C., Proud, S. R.,
565 Grainger, R. G.: Unveiling aerosol–cloud interactions – Part 1: Cloud contamination in satellite products
566 enhances the aerosol indirect forcing estimate, *Atmos. Chem. Phys.*, 17, 13151–13164, 2017.

567 Cohen, J., Screen, J. A., Furtado, J., C., et al.: Recent Arctic amplification and extreme mid-latitude weather, *Nat.*
568 *Geosci.*, 7(9), 627–637, 2014.

569 Coppo, P., Ricciarelli, B., Brandani, F., Delderfield, J., Ferlet, M., Mutlow, C., Munro, G., Nightingale, T., Smith,
570 D., Bianchi, S., Nicol, P., Kirschstein, S., Hennig, T., Engel, W., Frerick, J., Nieke, J., SLSTR: a high accuracy
571 dual scan temperature radiometer for sea and land surface monitoring from space, *J. Mod. Optic.*, 57(18), 1815-
572 1830, 2010.

573 Curry, J. A., Rossow, W. B., Randall, D., Schramm, J. L.: Overview of Arctic cloud and radiation characteristics. *J.*
574 *Climate*, 9, 1731–1764, 1996.

575 [Dybbroe, A.; Karlsson, K.-G.; Thoss, A. NWCSAF AVHRR cloud detection and analysis using dynamic thresholds
576 and radiative transfer modeling. Part II: Tuning and validation. *J. Appl. Meteorol.*, 44, 55–71, 2005.](#)

577 Derrien, M., Farki, B., Harang, L., Pochic, D., Sairouni, A., LeGldau, H., Noyalet, A.: Automatic Cloud Detection
578 Applied to NOAA-11/AVHRR Imagery, *Remote Sens. Environ.*, 46, 246-267, 1993.

579 Eck, T. F., B. N. Holben, J. S. Reid, O. Dubovik, A. Smirnov, N. T. O Neill, I. Slutsker, and S. Kinne, Wavelength
580 dependence of the optical depth of biomass burning, urban, and desert dust aerosols, *J. Geophys. Res.*, 104(1),
581 333-349, 1999.

582 Ghent, D. J., Corlett, G. K., Götttsche, F.-M., & Remedios, J. J.: Globalland surface temperature from the Along-
583 Track Scanning Radiometers, *J. Geophys. Res.*, 122, 12167–12193, 2017.

584 Gómez-Chova, L., Amorós-López, J., Mateo-García, G., Muñoz-Marí, J., Camps-Valls, G.: Cloud masking and
585 removal in remote sensing image time series, *J. Appl. Remote Sens.*, 11(1), 015005, 2017.

586 Hagolle, O., Sylvander, S., Huc, M., Claverie, M., Clesse, D., Dechoz, C., Lonjou, V., Poulain, V.: SPOT4 (Take5):
587 A simulation of Sentinel-2 time series on 45 large sites. *Remote Sens.*, 7, 12242–12264, 2015.

588 Hall, D. K., Riggs, G., Salomonson, V. V.: Algorithm Theoretical Basis Document (ATBD) for the MODIS snow
589 and sea-ice mapping algorithms, September 2001.

590 Holben, B. N., Eck, T. F., Slutsker, I., Tanre, D., Buis, J. P., Setzer, A., Vermote, E., Reagan, J. A., Kaufman, Y. J.,
591 Nakajima, T., Lavenu, F., Jankowiak, I., Smirnov, A.: AERONET - a federated instrument network and data
592 archive for aerosol characterization Remote Sens. Environ., 66, 1-16, 1998.

593 [Hollmann, R.; Merchant, C.J.; Saunders, R.; Downy, C.; Buchwitz, M.; Cazenave, A.; Chuvieco, E.; Defourny, P.;
594 de Leeuw, G.; Forsberg, R.; et al. The ESA climate change initiative Satellite Data Records for Essential Climate
595 Variables. Bull. Am. Meteorol. Soc., 94, 1541–1552, 2013.](#)

596 Istomina, L., Hoyningen-Huene, W., Kokhanovsky, A.A., Burrows, J.P.: The detection of cloud-free snow-covered
597 areas using AATSR measurements, Atmos. Chem. Phys., 9, 1279-1288, 2010.

598 Istomina, L.: Retrieval of aerosol optical thickness over snow and ice surfaces in the Arctic using Advanced Along
599 Track Scanning Radiometer, Ph.D. thesis, University of Bremen, Germany, 2012.

600 Kellogg, W. W.: Climatic feedback mechanisms involving the polar regions, Climate of the Arctic, Weller, G., and
601 Bowling, S. A., (Eds.), Geophysical Institute, University of Alaska, Fairbanks, AK, 111–116, 1975.

602 Key, J. and Barry, R. G.: Cloud cover analysis with Arctic AVHRR data. 1. Cloud detection, J. Geophys. Res., 94,
603 D15, 18521– 18535, 1989.

604 Kim B-M, Hong J-Y, Jun S-Y, Zhang X, Kwon H, Kim S-J, Kim J-H, Kim S-W and Kim H-K: Major cause of
605 unprecedented Arctic warming in January 2016: critical role of an Atlantic windstorm Sci. Rep., 7, 40051,
606 doi:10.1038/srep40051, 2017.

607 Khlopenkov, K., Trishchenko, A. SPARC: New cloud, snow, and cloud shadow detection scheme for historical 1-
608 km AVHRR data over Canada, J. Atmos. Ocean. Technol., 24, 322–343, 2007.

609 Klüser, L., Killius, N., Gesell, G.: APOLLO_NG – a probabilistic interpretation of the APOLLO legacy for AVHRR
610 heritage channels, Atmos. Meas. Tech., 8, 4155–4170, 2015.

611 Kokhanovsky, A. A.: Cloud Optics, Eds.: Mysak, L. A., Hamilton, K., Publ. Springer, 2006.

612 Kolmonen, P., Sundström, A. -M., Sogacheva, L., Rodriguez, E., Virtanen, T. H., & de Leeuw, G.: Uncertainty
613 characterization of AOD for the AATSR dual and single view retrieval algorithms, Atmos. Meas. Tech. Discuss.,
614 6, 4039–4075, 2013.

615 Kolmonen, P., Sogacheva, L., Virtanen, T. H., de Leeuw, G., Kulmala, M.: The ADV/ASV AATSR aerosol retrieval
616 algorithm: current status and presentation of a full-mission AOD dataset, Int. J. Digit. Earth, 9, 545-561, 2016.

617 Kotarba, A. Z.: A comparison of MODIS-derived cloud amount with visual surface observations, J. Atmos. Res., 92,
618 522–530, doi:10.1016/j.atmosres.2009.02.001, 2009.

619 Kotarba A. Z.: Inconsistency of surface-based (SYNOP) and satellite-based (MODIS) cloud amount estimations due
620 to the interpretation of cloud detection results. Int. J. Climatol. 37(11):4092–4104, 2017.

621 Law, K. S., Stohl, A.: Arctic Air pollution: origins and impacts, J. Science, 315 (5818), 1537-1540, doi:
622 10.1126/science.1137695, 2007.

623 Leese, J. A., Novak, C. S., Taylor, V. R.: The determination of cloud pattern motions from Geosynchronous Satellite
624 Image Data, J. Pattern Recognition, 2, 279-292, 1970.

625 Lyapustin, A., Wang, Y., and Frey, R.: An automated cloud mask algorithm based on time series of MODIS
626 measurements, J. Geophys. Res., 113, D16207, doi:10.1029/2007JD009641, 2008.

627 Lyapustin, A., Tedesco, M., Wang, Y., Aoki, T., Hori, M., Kokhanovsky, A.: Retrieval of snow grain size over
628 Greenland from MODIS Remote Sens. Environ., 113 (9), 1976-198, 2009.

629 Martins, J.V., Tanre, D., Remer, L., Kaufman, Y.J., Mattoo, S., Levy, R.: MODIS Cloud screening for remote
630 sensing of aerosols over oceans using spatial variability. Geophys. Res. Lett. 29 (12), 1619, 2002.

631 Mei, L., Xue, Y., Kokhanovsky, A. A., von Hoyningen-Huene, W., Istomina, L., de Leeuw, G., Burrows, J. P.,
632 Guang, J., Jing, Y., Aerosol optical depth retrieval over snow using AATSR data, International Journal of
633 Remote Sensing, 34, 5030-5041, 2013.

634 Mei, L., Rozanov, V. V., Vountas, M., Burrows, J. P., Levy, R. C., and Lotz, W. A.: Retrieval of aerosol optical
635 properties using MERIS observations: algorithm and some first results, Remote Sens. Environ., 197, 125–141,
636 2017a.

637 Mei, L. L., Vountas, M., Gómez-Chova, L., Rozanov, V., Jäger, M., Lotz, W., Burrows, J. P., and Hollmann, R.: A
638 Cloud masking algorithm for the XBAER aerosol retrieval using MERIS data, Remote Sens. Environ., 197, 141–
639 160, 2017b.

640 [Meerkötter, R., König, C., Bissolli, P., Gesell, G., Mannstein, H., A 14-year European cloud climatology from
641 NOAA/AVHRR data in comparison to surface observations. Geophys. Res. Lett., 31,
642 doi:10.1029/2004GL020098, 2004.](#)

643 ~~Meyer, K., Platnick, S.: Utilizing the MODIS 1.38 μm channel for cirrus cloud optical thickness retrievals:
644 Algorithm and retrieval uncertainties, J. Geophys. Res., 115, D24209, 2010.~~

645 Minnis, P., Spangenberg, D.A., Chakrapani, V.: Distribution and validation of cloud cover derived from AVHRR
646 data over the Arctic Ocean during the SHEBA year. Proc. 13th ARM Science Team Meeting, Broomfield,
647 Colorado, March 31–April 4, 2003.

648 Musial, J. P., Husler, F., Sutterlin, M., Neuhaus, C., Wunderle, S.: Daytime low Stratiform cloud detection on
649 AVHRR Imagery, Remote Sens., 6, 5124-5150, doi: 10.3390/rs6065124, 2014.

650 North, P. R. J., Briggs, S. A., Plummer, S. E., & Settle, J. J.: Retrieval of land surface bidirectional reflectance and
651 aerosol opacity from ATSR-2 multi-angle imagery, IEEE Trans. Geosci. Remote Sens. 37, 526–537, 1999.

652 Pavolonis, M. J., Heidinger, A. K., and Uttal, T.: Daytime global cloud typing from AVHRR and VIIRS: Algorithm
653 description, validation, and comparison, J. Appl. Meteorol., 44, 804-826, 2005.

654 Pearson, K., VII. Mathematical contributions to the theory of evolution.—III. Regression, heredity, and panmixia,
655 Philos. T. Roy. Soc. A., 187, 253-318, 1896.

656 Pithan, F., Mauritsen, T.: Arctic amplification dominated by temperature feedbacks in contemporary climate models,
657 Nat. Geosci., 7, 181–184, 2014.

658 Platnick, S., Fontenla, J. M.: Model calculations of solar spectral irradiance in the 3.7 band for Earth remote sensing
659 application, Am. Meteorol. Soc., 47, 124-134, 2008.

660 Remer, L. A., Mattoo, S., Levy, R. C., Heidinger, A., Pierce, R. B., Chin, M.: Retrieving aerosol in a cloudy
661 environment: aerosol product availability as a function of spatial resolution, Atmos. Meas. Tech., 5, 1823–1840,
662 2012.

663 Rodgers, J. L., Nicewander, W. A.: Thirteen Ways to Look at the Correlation Coefficient, *The American*
664 *Statistician*, 42 (1), 59-66, 1988.

665 Rosenfeld, D., Cattani, E., Melani, S., Levizzani, V.: Considerations on daylight operation of 1.6 versus 3.7 mm
666 channel on NOAA and METOP satellites, *American Meteorologica Society*, 85, 873-881, 2004.

667 Rossow, W.B., and Garder, L. C.: Validation of ISCCP cloud detections. *J. Climate*, 6, 2370-2393, 1993.

668 Serreze M. C., Barry R. G.: Processes and impacts of Arctic amplification: a research synthesis, *Global and*
669 *Planetary Change*, 77, 85–96, 2011.

670 Meirink, J., F., van Zadelhoff, G. J., Algorithm Theoretical Basis Document SEVIRI Cloud Physical Products,
671 CLAAS Edition 2, Date: 10.06.2016, Issue: 2.2. 2016.

672 Shi, Y., Zhang, J., Reid, J. S., Liu, B., and Hyer, E. J.: Critical evaluation of cloud contamination in the MISR
673 aerosol products using MODIS cloud mask products, *Atmos. Meas. Tech.*, 7, 1791– 1801, doi:10.5194/amt-7-
674 1791-2014, 2014.

675 Sobrino, J. A., Jiménez-Muñoz, J. C., Sòria, G., Ruescas, A. B., Danne, O., Brockmann, C., Ghent, D., Remedios, J.,
676 North, P., Merchant, C., Berger, M., Mathieu, P. P., Göttsche, F. M.: Synergistic use of MERIS and AATSR as a
677 proxy for estimating Land Surface Temperature from Sentinel-3 data, *Remote Sens. Environ.*, 179, 149–161,
678 2016.

679 Sobrino, J. A., Jiménez-Muñoz, J. C., Barres, G. S., Julien, Y.: Synergistic Use of The Sentinel Missions For
680 Estimating And Monitoring Land Surface Temperature (SEN4LST FINAL REPORT), ESA technical report, doi:
681 10.13140/RG.2.2.34693.35049, 2013.

682 Soliman, A., Duguay, C., Saunders, W., Hachem, S.: Pan-Arctic land surface temperature from MODIS and
683 AATSR: Product development and intercomparison, *Remote. Sens-Basel*, 4, 3833-3856, 2012.

684 Spangenberg, D. A., Chakrapani, V., Doelling, D. R., Minnis, P., and Arduini, R. F.: Development of an automated
685 Arctic cloud mask using clear-sky satellite observations taken over the SHEBA and ARM NSA sites, *Proc. 6th*
686 *Conf. on Polar Meteor. and Oceanography*, San Diego, CA, 14–18 May 2001, 246–249, 2001.

687 Thomas, G. E., Carboni, E., Sayer, A. M., Poulsen, C. A., Siddans, R., and Grainger, R. G.: Oxford-RAL Aerosol
688 and Cloud (ORAC): aerosol retrievals from satellite radiometers, in: *Satellite Aerosol Remote Sensing Over*
689 *Land*, edited by: Kokhanovsky, A. A. and de Leeuw, G., Springer, Berlin, Germany, 193–225, 4042, 4051, 2009.

690 Várnai, T., Marshak, A.: Effect of Cloud Fraction on Near-Cloud Aerosol Behavior in the MODIS Atmospheric
691 Correction Ocean Color Product, *Remote Sens.*, 7, 5283–5299, 2015.

692 ~~Veefkind, J. P., & de Leeuw, G.: A new algorithm to determine the spectral aerosol optical depth from satellite~~
693 ~~radiometer measurements., *J. Aerosol Sci.* 29, 1237–1248, 1998.~~

694 ~~Veefkind, J. P., de Leeuw, G. D., and Durkee, P. A.: Retrieval of aerosol optical depth over land using two angle~~
695 ~~view satellite radiometry during TARFOX, *Geophys. Res. Lett.*, 25, 3135–3138, 1999.~~

696 Werkmeister, A., Lockhoff, M., Schrempf, M., Tohsing, K., Liley, B., and Seckmeyer, G.: Comparing satellite- to
697 ground-based automated and manual cloud coverage observations – a case study, *Atmos. Meas. Tech.*, 8, 2001-
698 2015, 2015.

699 Wendisch, M., M. Brückner, J. P. Burrows, S. Crewell, K. Dethloff, K. Ebell, Ch. Lüpkes, A. Macke, J. Notholt, J.
700 Quaas, A. Rinke, and I. Tegen,: Understanding causes and effects of rapid warming in the Arctic. *Eos*, 98, doi:
701 10.1029/2017EO064803, 2017.

702 Wind, G., da Silva, A. M., Norris, P. M., Platnick, S., Mattoo, S., Levy, R. C.: Multi-sensor cloud and aerosol
703 retrieval simulator and remote sensing from model parameters – Part 2: Aerosols, *Geosci. Model Dev.*, 9, 2377–
704 2389, 2016.

705 WMO: Manual on Codes. Part A – Alphanumeric Codes. Secretariat of the World Meteorological Organization:
706 Geneva, Switzerland, 1995.

707 Zavody, A. M., Mutlow, C. T., and Llewellyn-Jones, D. T.: Cloud Clearing over the Ocean in the Processing of Data
708 from the Along-Track Scanning Radiometer (ATSR), *Journal of Atmospheric and Oceanic Technology*, 17, 595-
709 615, 2000.

Table 1. Calculation of cloudiness in percentage for corresponding okta values

Percentage of Cloud	Okta
0	0
$0 < \% < 18.75$	1
$18.75 \leq \% < 31.25$	2
$31.25 \leq \% < 43.75$	3
$43.75 \leq \% < 56.25$	4
$56.25 \leq \% < 68.75$	5
$68.75 \leq \% < 81.25$	6
$81.25 \leq \% < 100$	7
100	8

Table 2. Simulated and observed reflectance values at 3.7 μm (Allen et al., 1990)

Surface/cloud Type	Simulation of 3.7 μm Reflectance	Observation of 3.7 μm Reflectance
Ice cloud	0.01-0.3	0.02-0.27
Liquid cloud	0.1-0.45	0.08-0.36
Clear land	~0.15	0.03-0.1
Snow cover	0.005-0.025	0.02- 0.04

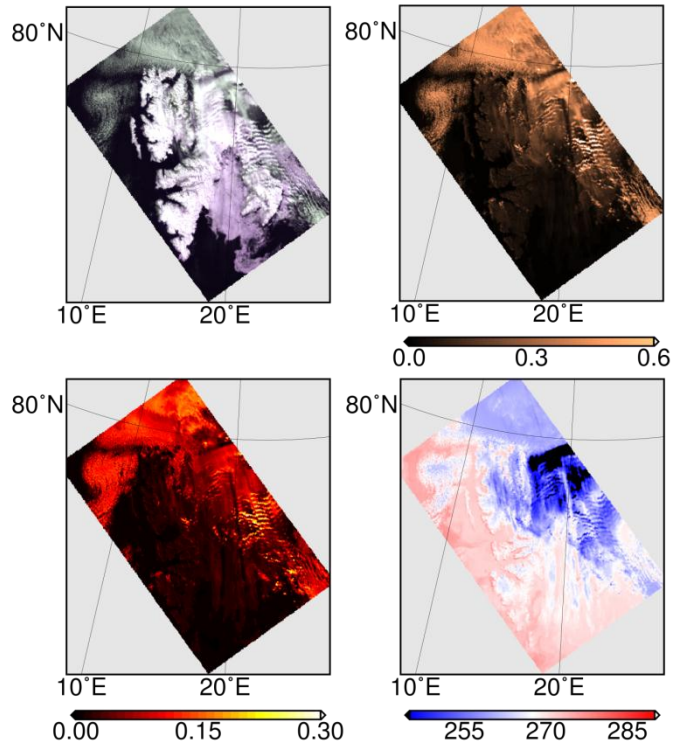
Table 3. Land classification criteria in cloud-free scene.

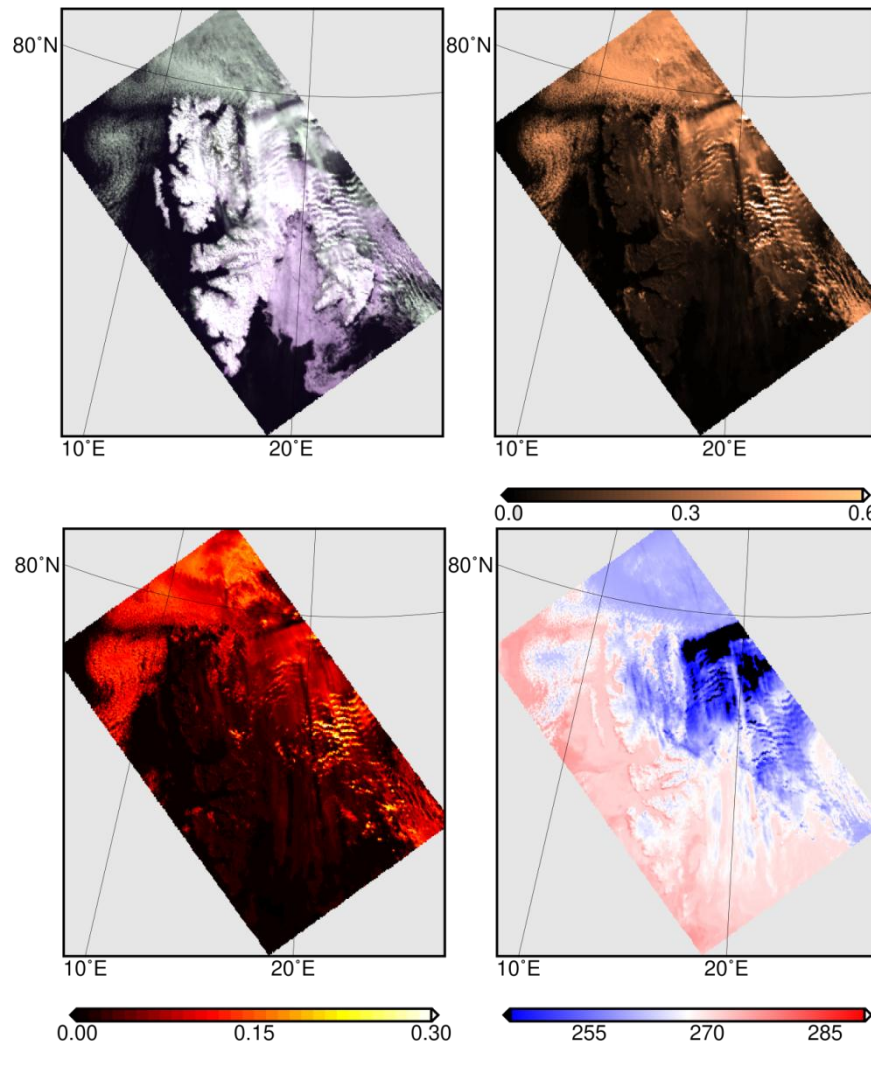
Surface Type	Test Simulation of 3.7 μm Reflectance	Description
Water	$R_{0.87} < 11\% \ \& \ \text{NDSI} \geq 0.4$	MODIS snow and ice mapping ATBD
Sea-ice	$R_{0.87} > 11\% \ \& \ \text{NDSI} \geq 0.4$	(Hall et al., 2001)
Land	$R_{3.7} > 0.04 \ \& \ R_{0.66} < 0.2 \ \ \text{NDSI} < 0.4$	Allen et al., 1999
Snow	$R_{3.7} \leq 0.04$	Allen et al., 1999

713
714

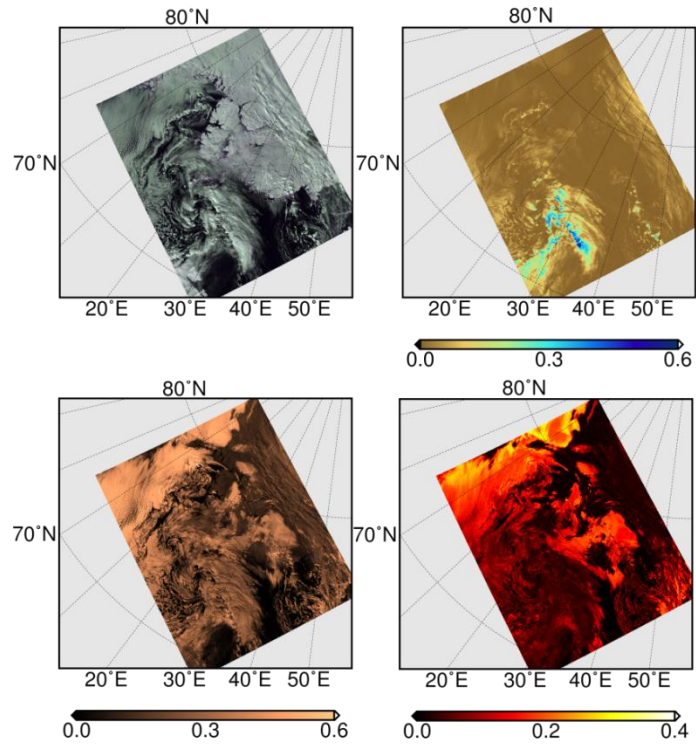
Table 4. A summary of the comparison of ASCIA and ESA cloud product with SYNOP measurements used to validate these products.

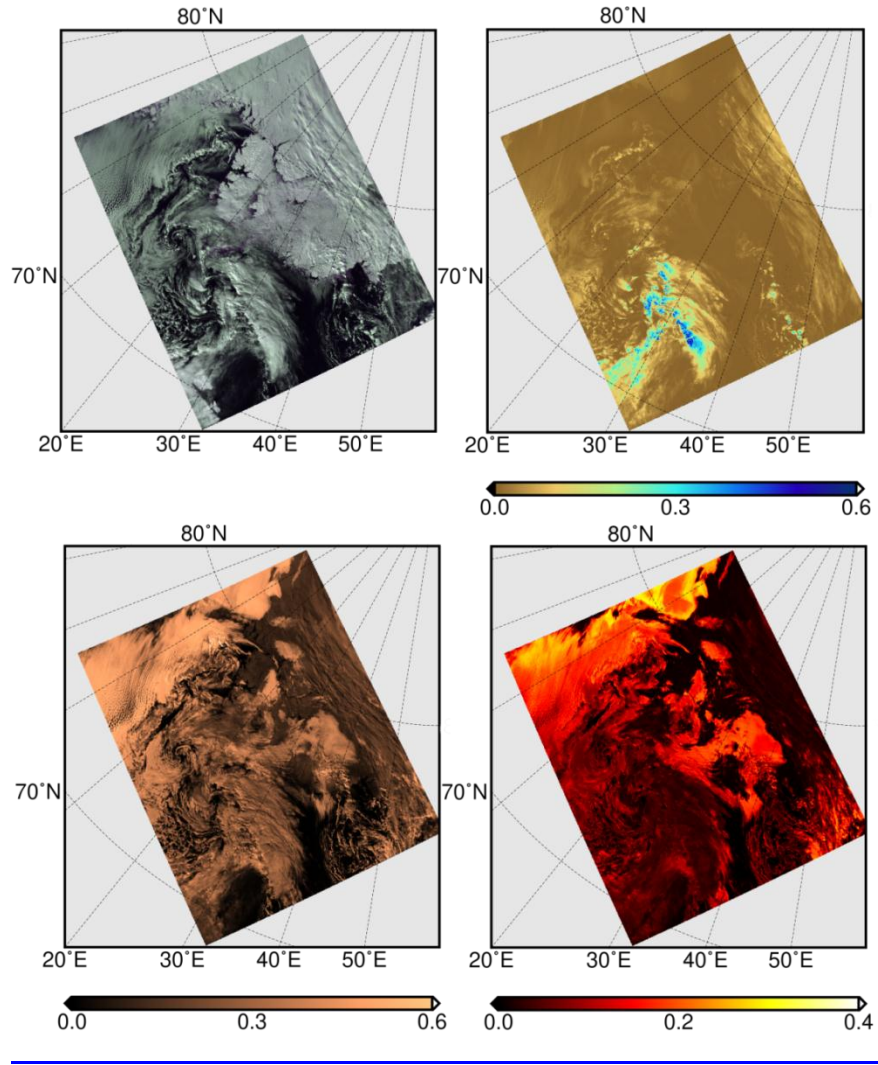
Cloud data	Criteria	
	within ± 2 oktas	within ± 1 okta
ASCIA vs. SYNOP	96 % correct agreement 4 % incorrect disagreement	83 % correct agreement 17 % incorrect disagreement
ESA vs. SYNOP	68 % correct agreement 32 % incorrect disagreement	50 % correct agreement 50 % incorrect disagreement



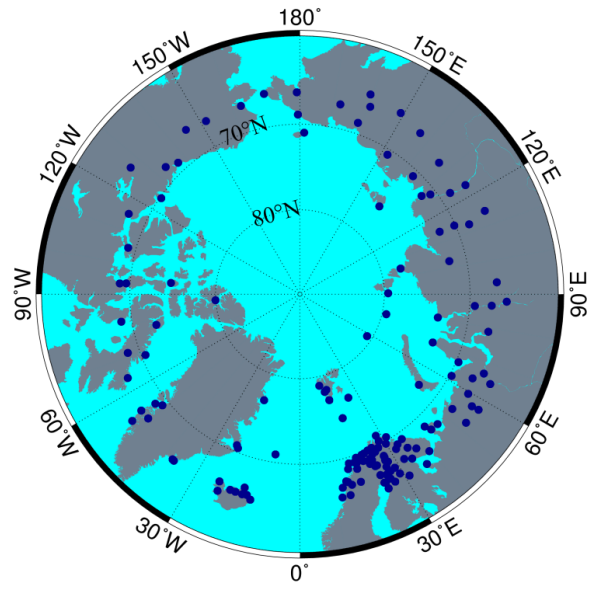


715 **Figure 1.** Upper left: the false colour RGB image of AATSR (using 0.67, 0.87 and 0.55 μm channels) over Svalbard, 10 May
 716 2006, upper right: 1.6 μm reflectance, lower left: 3.7 μm reflectance, lower right: 11 μm brightness temperature.

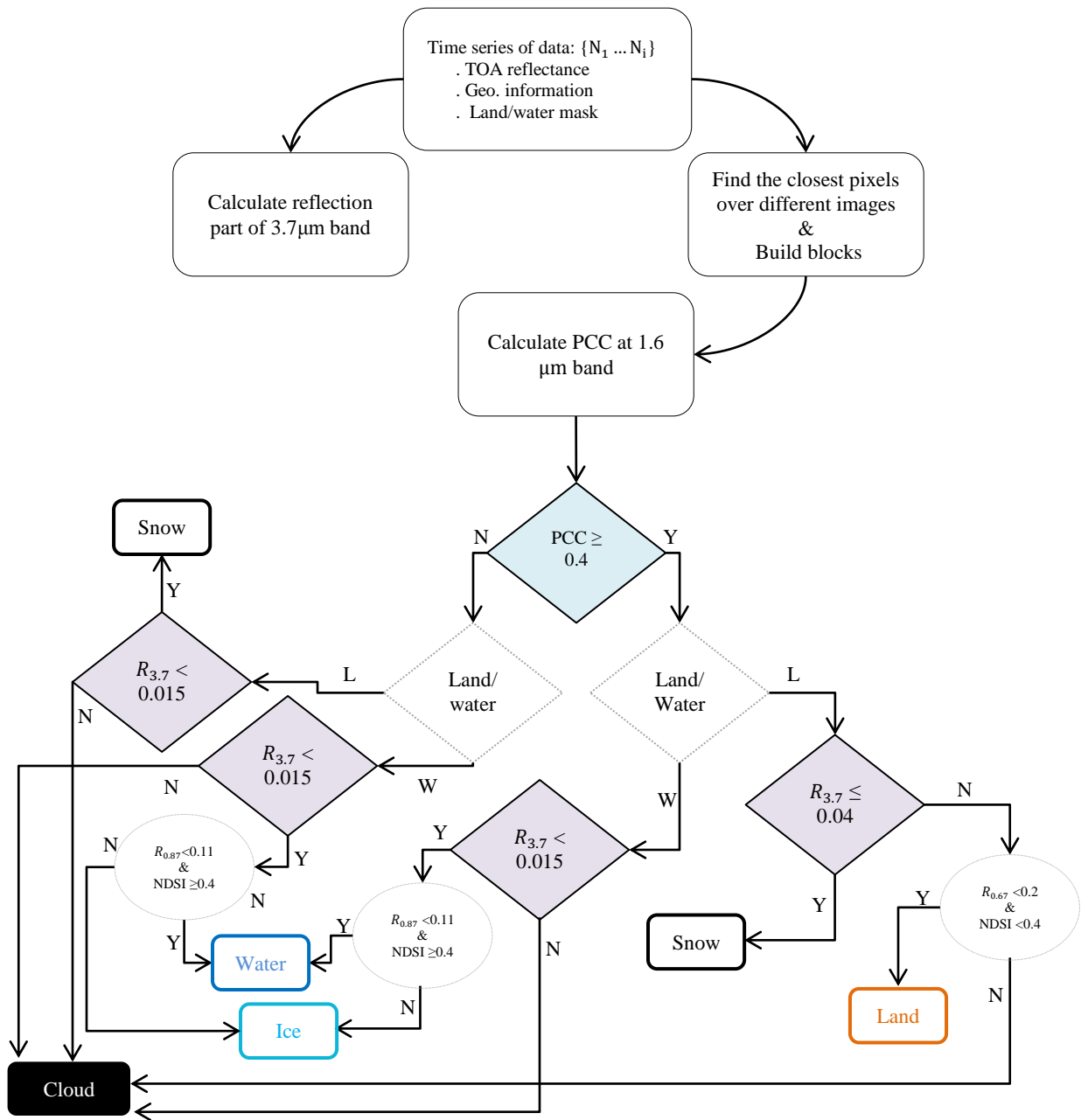




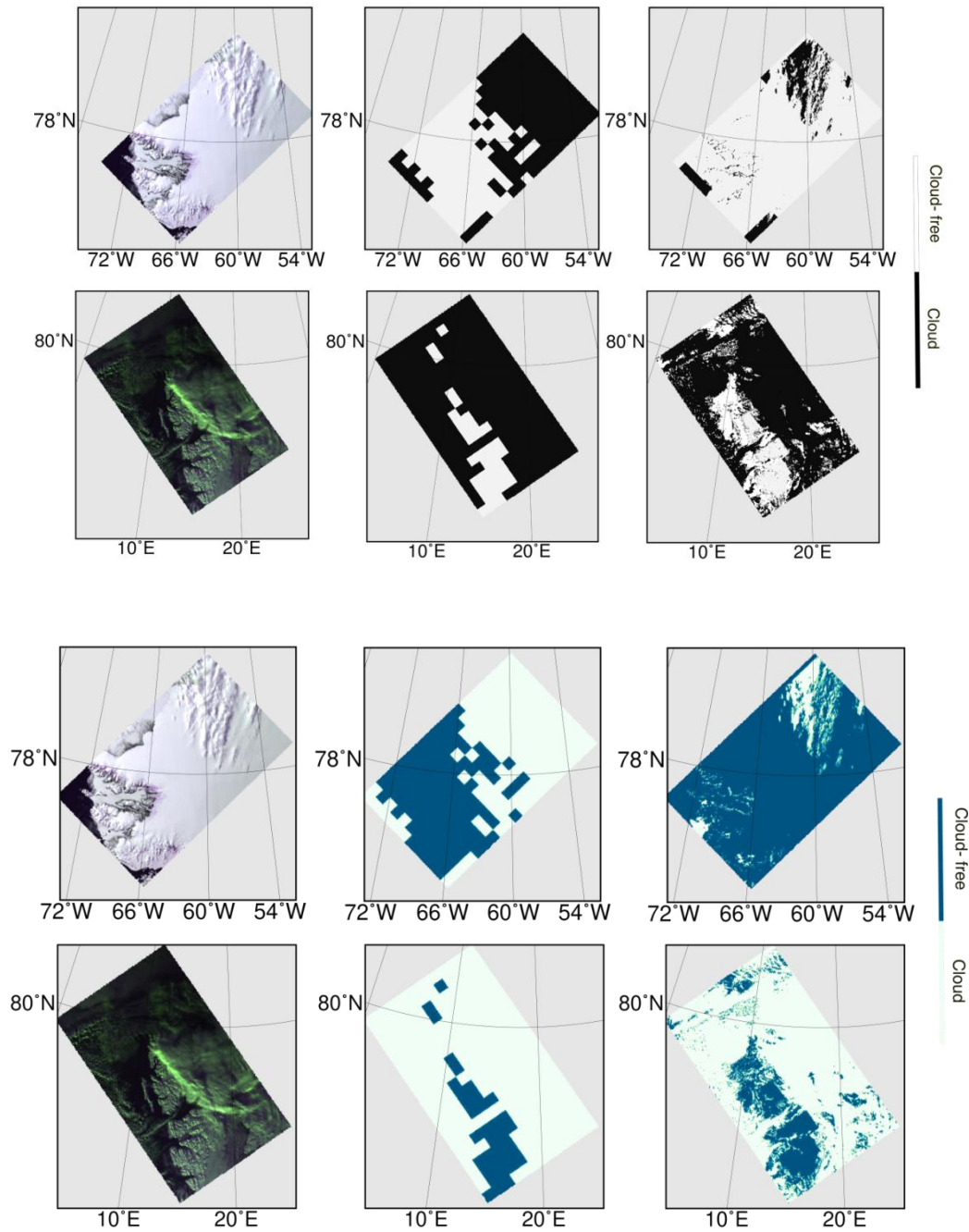
717 **Figure 2.** Upper left: the RGB [false colour](#) image ([using 0.67, 0.87 and 0.55 μm channels](#)) of SLSTR over Svalbard, 18
 718 April 2017, upper right: 1.37 μm reflectance, lower left: 1.6 μm reflectance, lower right: 3.7 μm reflectance.



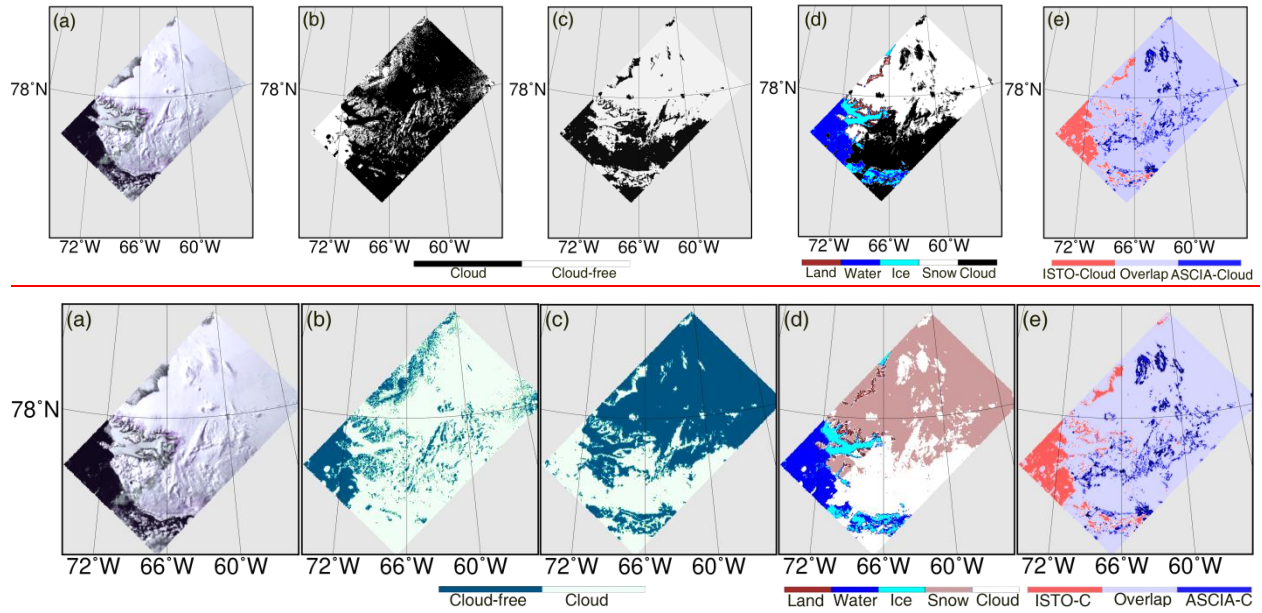
719 **Figure 3.** SYNOP network coverage over the Arctic, the dark blue points indicate the location of SYNOP stations.



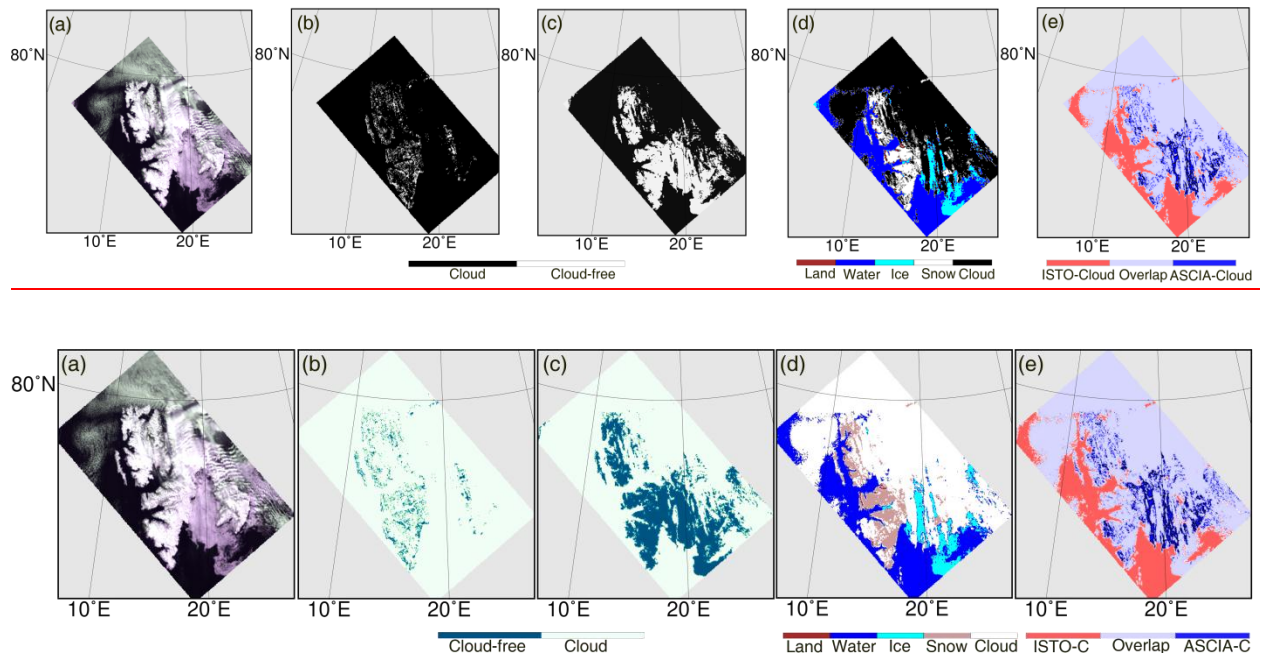
720 **Figure 4.** The schematic flowchart of ASCIA.



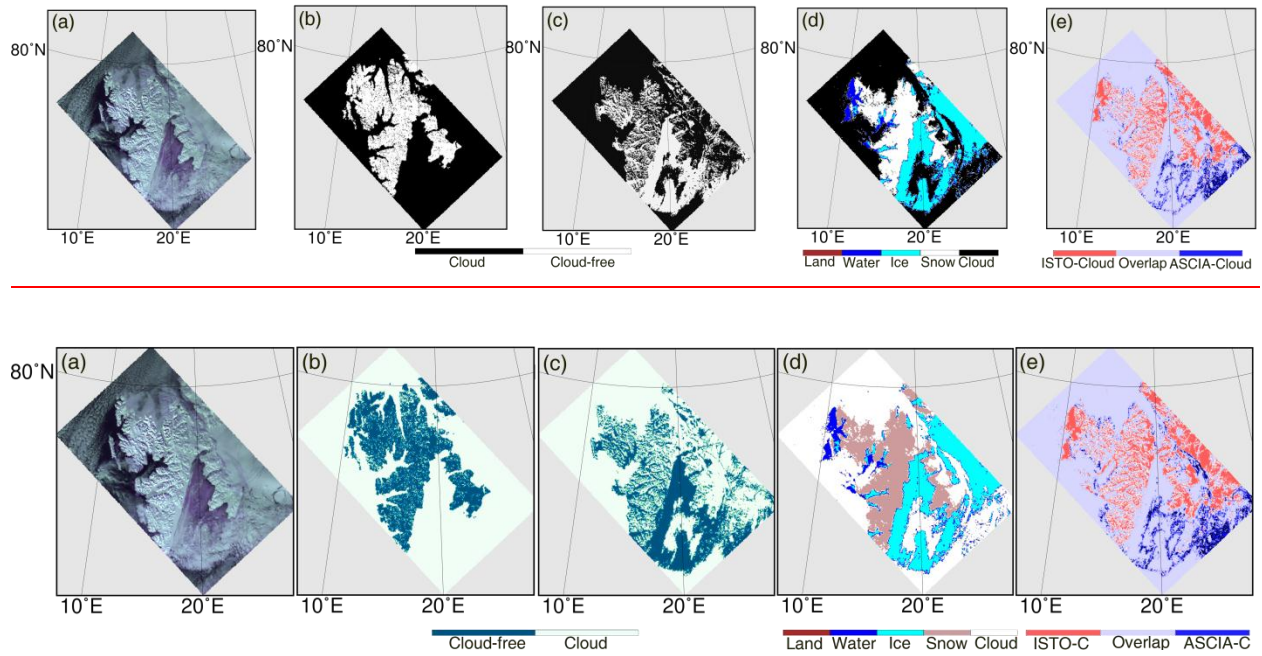
721 **Figure 5.** Examples of the results of ASCIA on AATSR observations on the scenes over Greenland (upper panels) [between](#)
 722 [\(75°N, 48°W\), \(75°N, 75°W\), \(81°N, 48°W\), \(81°N, 75°W\)](#), taken on the 18 May 2008 and Svalbard (lower panels), within
 723 [\(75°N, 4°E\), \(75°N, 32°E\), \(81°N, 4°E\), \(81°N, 32°E\)](#) (Lower panels), taken on the 18 May 2008 and on the 1 March 2008
 724 [respectively](#). Left panels: RGB false colour images (using 0.67, 0.87 and 0.55 μm channels), middle panels: Cloud detection at
 725 block level ($25 \times 25 \text{ km}^2$), right panels: cloud detection at scene level.



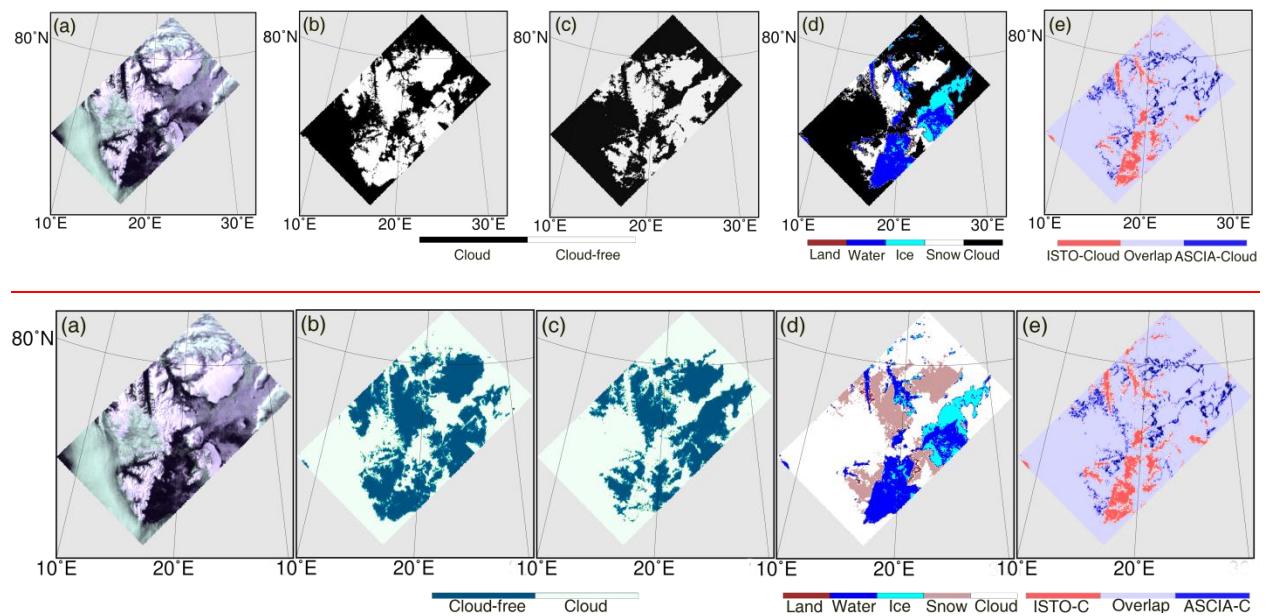
726 | **Figure 6.** (a) The RGB [false colour](#) image (using 0.67, 0.87 and 0.55 μm channels) of AATSR over northern Greenland, 24 May
 727 | 2008, (b) Nadir cloud flag from AATSR L2 product, (c) cloud detection based on spectral shape of clear snow, (d) cloud
 728 | detection of ASCIA, (e) difference between ISTO and ASCIA



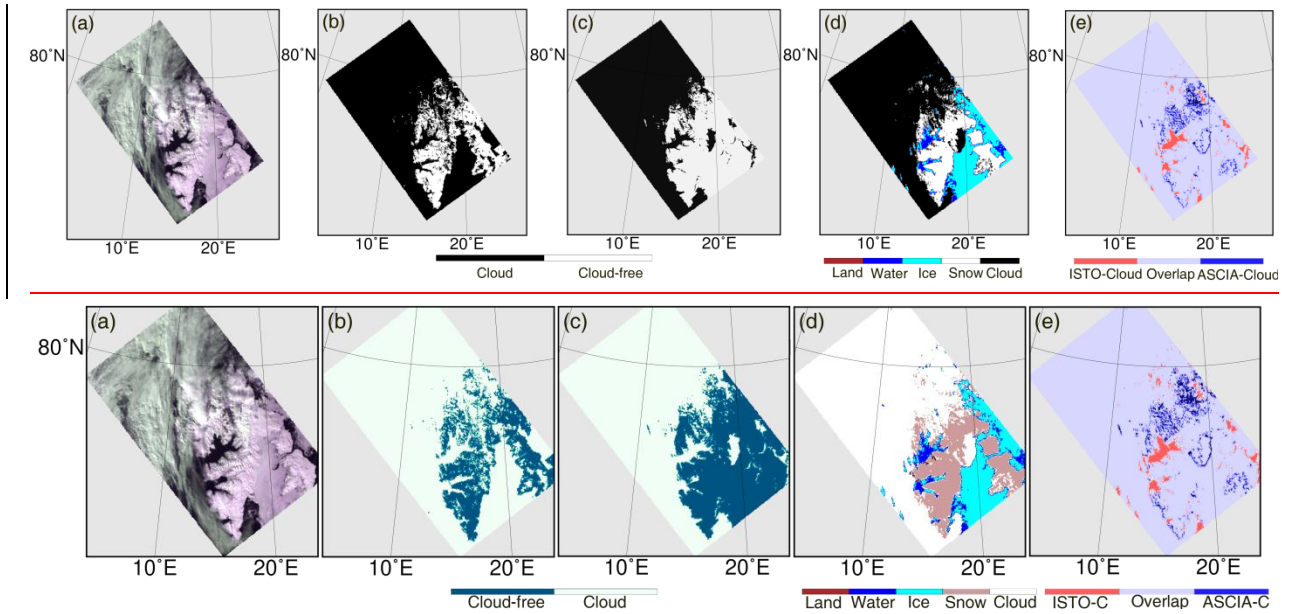
729 | **Figure 7.** (a) The RGB [false colour](#) image (using 0.67, 0.87 and 0.55 μm channels) of AATSR over Svalbard, 10 May 2006, (b)
 730 | Nadir cloud flag from AATSR L2 product, (c) cloud detection based on spectral shape of clear snow, (d) cloud detection of
 731 | ASCIA, (e) difference between ISTO and ASCIA.



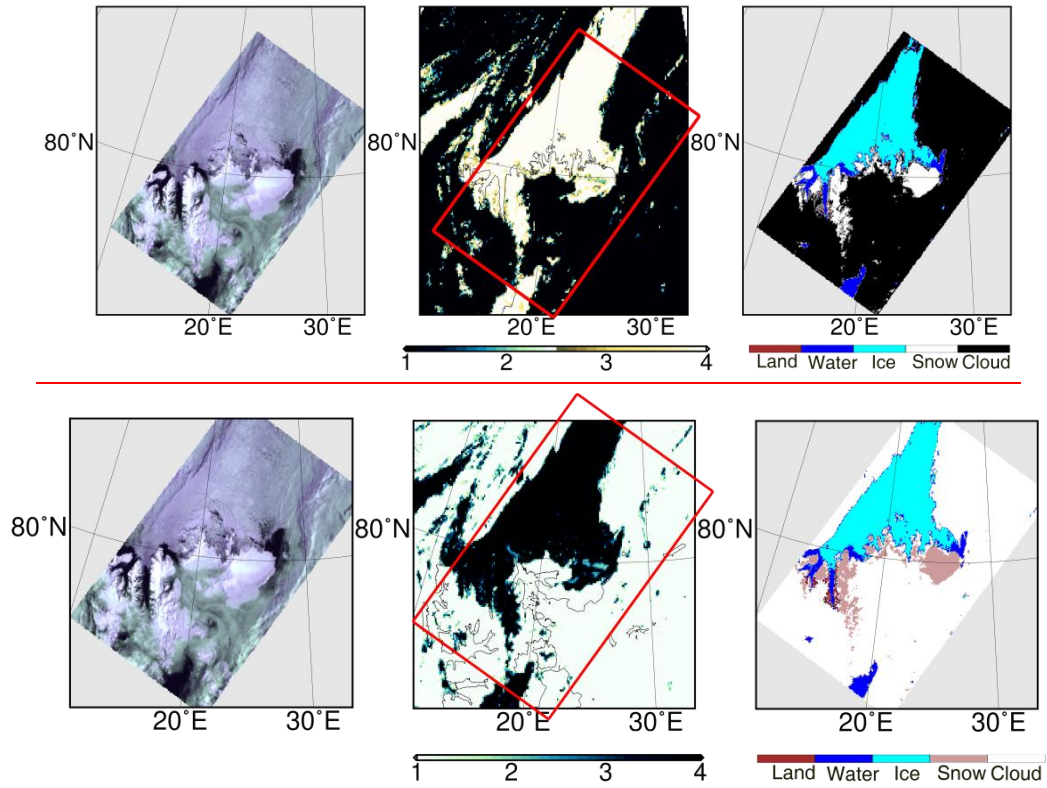
732 **Figure 8.** (a) The RGB false colour image (using 0.67, 0.87 and 0.55 μm channels) of AATSR over Svalbard, 18 March 2008, (b) Nadir
 733 cloud flag from AATSR L2 product, (c) cloud detection based on spectral shape of clear snow, (d) cloud detection of ASCIA, (e) difference
 734 between ISTO and ASCIA.



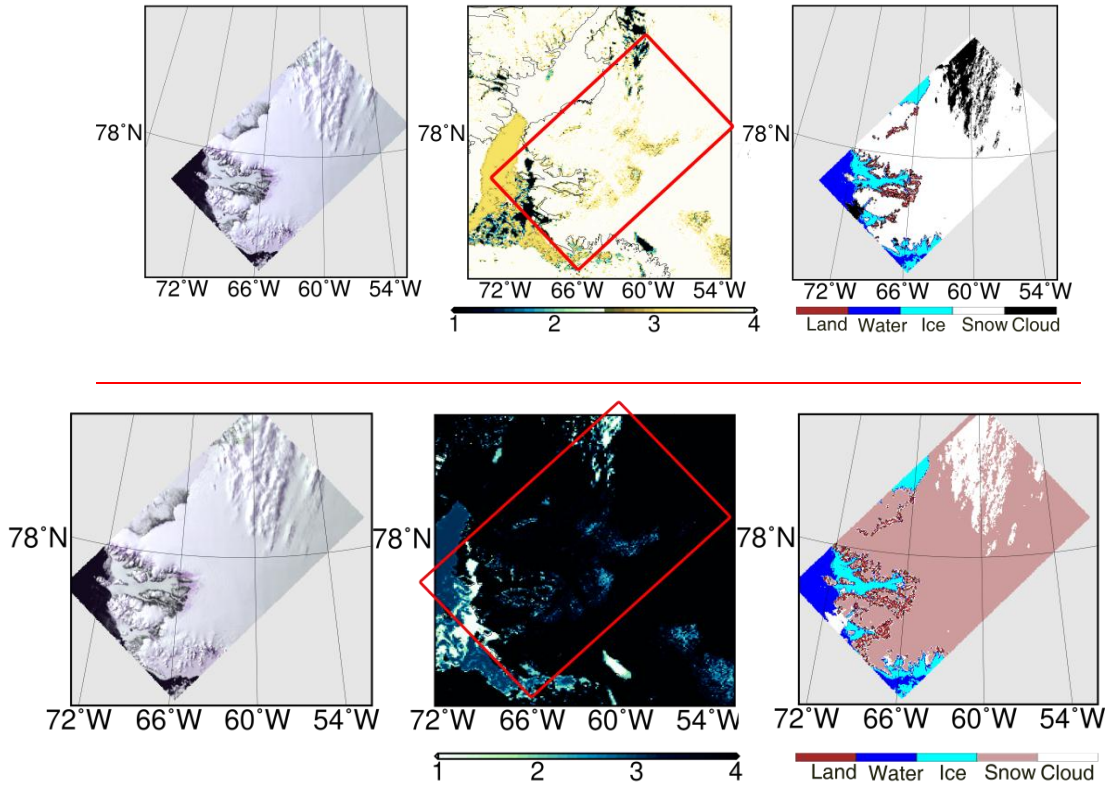
735 **Figure 9.** (a) The RGB false colour image (using 0.67, 0.87 and 0.55 μm channels) of AATSR over Svalbard, 6 July 2008, (b) Nadir
 736 cloud flag from AATSR L2 product, (c) cloud detection based on spectral shape of clear snow, (d) cloud detection of ASCIA, (e) difference
 737 between ISTO and ASCIA.



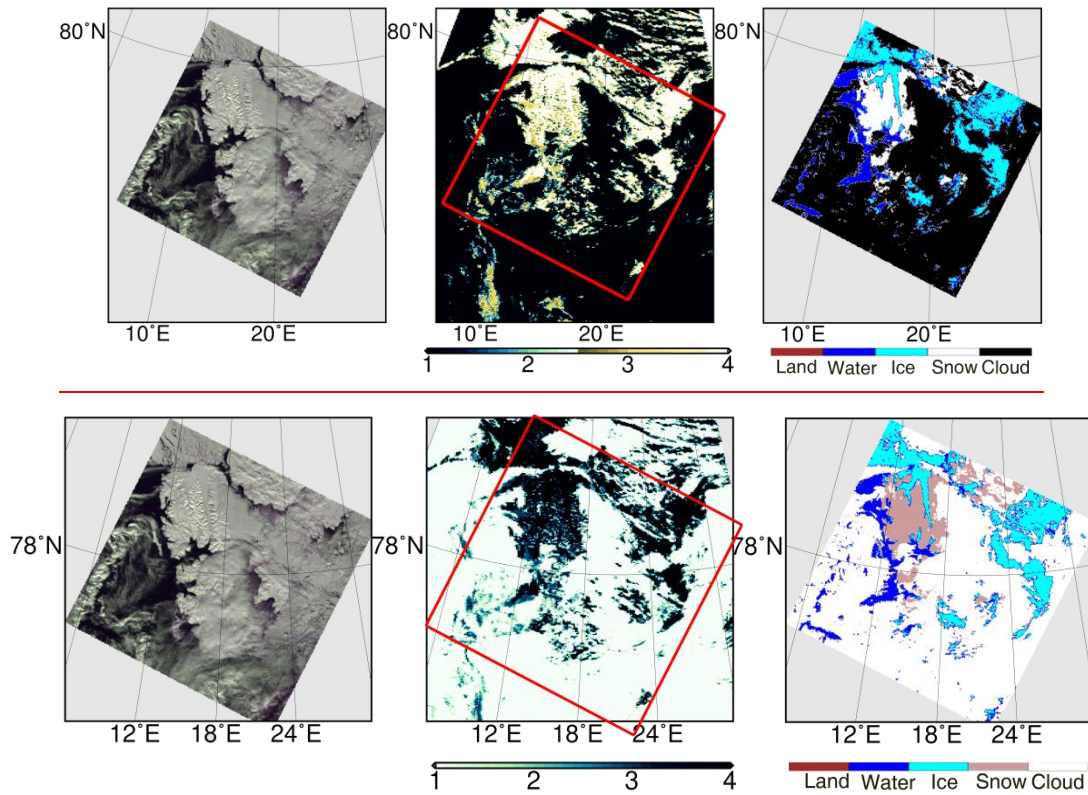
739 **Figure 10.** (a) The RGB false colour image (using 0.67, 0.87 and 0.55 μm channels) of AATSR over Svalbard, 3 May 2006, (b) Nadir cloud
 740 flag from AATSR L2 product, (c) cloud detection based on spectral shape of clear snow, (d) cloud detection of ASCIA, (e) difference between
 741 ISTO and ASCIA.



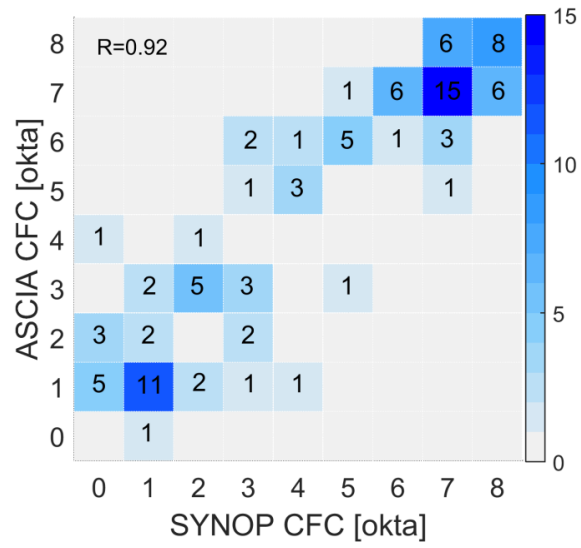
742 | **Figure 11.** Left panel: RGB false colour image (using 0.67, 0.87 and 0.55 μm channels) of AATSR over Svalbard, 14 July
 743 2008, 16h 40min 45s, middle panel MODIS cloud mask algorithm retrieved data: 1- cloudy, 2- probably cloudy, 3- probably
 744 clear, 4- clear, (red rectangle shows the coverage of AATSR) for 16h 25 min, right panel: the results for the cloud detection of
 745 ASCIA.



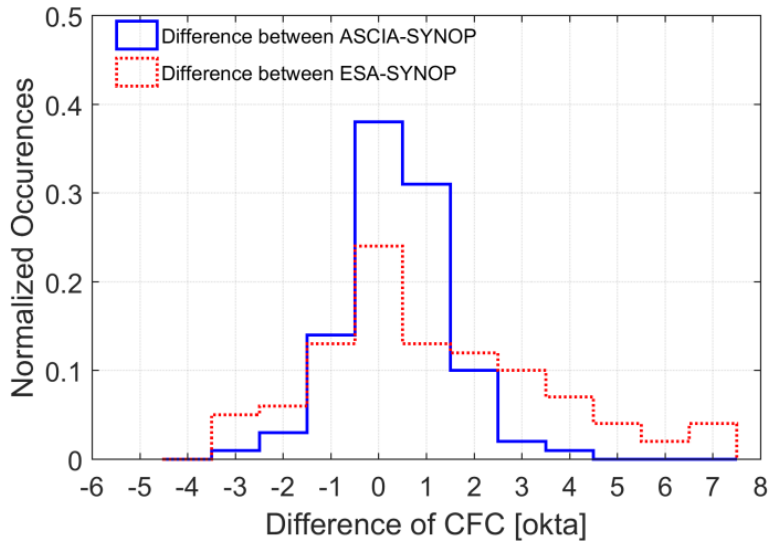
746 | **Figure 12.** Left panel: RGB [false colour](#) image ([using 0.67, 0.87 and 0.55 \$\mu\text{m}\$ channels](#)) -of AATSR over Greenland, 18 May
 747 2008, 23h 13min 38s, middle panel: MODIS cloud mask: 1- cloudy, 2- probably cloudy, 3- probably clear, 4- clear, (red
 748 rectangle shows the coverage of AATSR) for 23h 5min, right panel: Cloud detection of ASCIA.



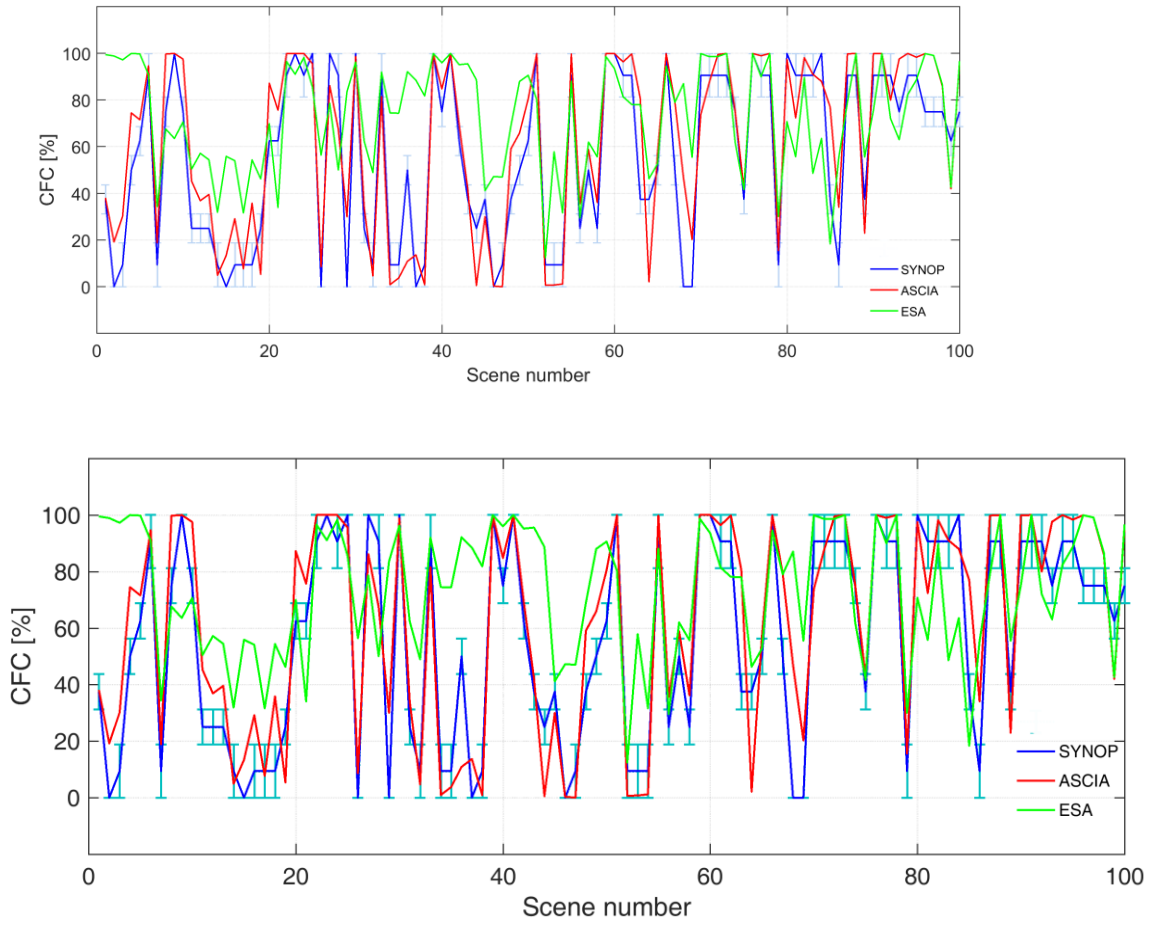
749 | **Figure 13.** Left panel: The RGB [false colour](#) image ([using 0.67, 0.87 and 0.55 \$\mu\text{m}\$ channels](#)) of SLSTR over Svalbard, 18 April
 750 | 2017, 10hr 15min 6s, Middle panel: MODIS cloud mask: 1- cloudy, 2- probably cloudy, 3- probably clear, 4- clear, (red rectangle
 751 | shows the coverage of AATSR) for 11h 30m, right panel: Cloud detection of ASCIA.



752 **Figure 14.** Density plot of occurrences of the CFC by ASCIA as a function of SYNOP.



753 **Figure 15.** Histogram of CFC differences (blue: ASCIA minus SYNOP; red: ESA cloud product minus SYNOP).



754 **Figure 16.** CFC in percent by ASCIA (red), SYNOP (blue) and ESA Cloud Product (green) for 100 scenarios of March, May and
 755 July 2008 over Svalbard and Greenland. Light blue error bars show the range of percentage values for each okta from SYNOP
 756 measurements.